

OPEN ACCESS

Review—Polymer Electrolytes for Magnesium Batteries: Forging Away from Analogs of Lithium Polymer Electrolytes and Towards the Rechargeable Magnesium Metal Polymer Battery

To cite this article: Bumjun Park and Jennifer L. Schaefer 2020 J. Electrochem. Soc. 167 070545

View the <u>article online</u> for updates and enhancements.





Review—Polymer Electrolytes for Magnesium Batteries: Forging Away from Analogs of Lithium Polymer Electrolytes and Towards the Rechargeable Magnesium Metal Polymer Battery

Bumjun Park and Jennifer L. Schaefer*, 2 (1)

Department of Chemical and Biomolecular Engineering, University of Notre Dame, Notre Dame, Indiana 46556, United States of America

Batteries based on alternatives to lithium are now of global research interest. Magnesium metal batteries are particularly attractive for their potential high energy density. Polymer electrolytes for high density rechargeable batteries have been sought for decades, due to their improved thermal stability compared with liquids and their lower density and cost compared with inorganic solids. Yet, little success has so far been realized in polymer electrolytes for magnesium metal batteries. In this review, the magnesium polymer electrolyte literature is comprehensively explored. Differences between requirements for lithium polymer and magnesium polymer batteries are discussed as well as the consequences on necessary considerations for impactful magnesium polymer electrolyte research.

© 2020 The Author(s). Published on behalf of The Electrochemical Society by IOP Publishing Limited. This is an open access article distributed under the terms of the Creative Commons Attribution 4.0 License (CC BY, http://creativecommons.org/licenses/by/4.0/), which permits unrestricted reuse of the work in any medium, provided the original work is properly cited. [DOI: 10.1149/1945-7111/ab7c71]

Manuscript submitted January 3, 2020; revised manuscript received February 24, 2020. Published March 30, 2020. This paper is part of the JES Focus Issue on Challenges in Novel Electrolytes, Organic Materials, and Innovative Chemistries for Batteries in Honor of Michel Armand.

Research in "beyond lithium" rechargeable electrochemical energy storage systems based on alternative active ions has gained steam in the past decade. Magnesium, as the lightest of the multivalent metals considered practical for battery applications (beryillium is notably toxic and rarer), offers attractively high charge capacity of 3833 mAh cm⁻³ and 2205 mAh g⁻¹, compared with 2046 mAh cm⁻³ and 3862 mAh g⁻¹ for Li metal and 760 mAh cm⁻³ and 372 mAh g⁻¹ for lithiated graphite. days make the state of the state o 8th most abundant element in the Earth's crust, the 3rd most abundant element in seawater, and significantly more geographically widespread than lithium.³⁻⁷ As noted by several research review articles, rechargeable magnesium-based batteries with magnesium metal anodes make the most sense to pursue; lower energy density magnesium-ion formats employing intercalation or conversion anodes are unlikely to be competitive with alternatives based on sodium (Fig. 1). ^{2,3,7-10} Thus, recent research on magnesium electrolytes has focused on compatibility with Mg metal anodes while achieving other favorable properties.^{2-4,7-9,11-14} The Mg metal anode is hypothesized to be less likely to show dendritic growth than the Li metal anode due to the thermodynamic properties of Mg metal which prefer three dimensional crystal growth rather than one dimensional dendritic growth, ^{15–18} however, Mg dendritic growth has been reported in several liquid electrolytes. ^{19–22} Thus, dendritic growth still remains a potential obstacle for utilizing the Mg metal anode.

Researchers have pursued polymer electrolytes for use with metal anodes for decades. Polymer electrolytes are advantageous for lower cost and easier processibility compared with inorganic solid-state electrolytes along with improved thermal and mechanical stability, and potentially electrochemical stability, compared with liquid electrolytes. We highlight the seminal contributions by Michel Armand, to whom the focus issue that this article appears in honors, to the polymer electrolyte field. ^{23–26} The materials and methods for lithium polymer electrolytes have been widely researched. ^{23–34} Those materials and methods are also used for mangesium conducting polymer electrolytes, but with little success. ³⁵ The distinct differences between the magnesium and lithium systems, such as stronger interaction of the magnesium cation (Mg²⁺) with counter ions or polymer hosts, higher under/overpotentials for Mg

electrodeposition/dissolution, and nature of the anode-electrolyte interface, mean that new materials and evaluation techniques are required for impactful advances in magnesium polymer electrolytes. Necessary properties of the magnesium polymer electrolyte include:

- \bullet Adequate conduction of magnesium, either as Mg^{2+} or, more likely, a complex such as MgA^+
- Chemical and electrochemical stability against the relevant electrodes, most importantly the Mg metal anode
- Facilitation of non-dendritic and high Coulombic efficiency Mg metal electrodeposition and electrodissolution at low underpotentials and overpotentials
- Other properties commonly desired from a polymer electrolyte, including adequate electrochemical stability windows, low interfacial impedance, high thermal stability, sufficient mechanical properties, and negligible electronic conductivity

In this review, prior work on magnesium polymer electrolytes is compiled and the details of material evaluation are highlighted, with a special emphasis placed on the attributes most important for magnesium metal polymer batteries. The molecular structures of materials used in prior magnesium polymer electrolytes, including polymers, solvents, and ionic liquids, are displayed in Fig. 2 for reference.

Compatibility of Common Solvents and Magnesium Salts with Magnesium Metal

Due to the higher reduction potential of Mg²⁺ (about 0.7 V higher than Li⁺/Li) and reduced reactivity of Mg metal compared with the alkali metals, there exist a greater number of materials that are electrochemically stable at the relevant magnesium anode operating potential as well as chemically stable in contact with Mg metal. For example, ethereal solvents, sulfoxides, and sulfones are believed to be chemically and electrochemically stable against Mg metal, allowing for a pristine electrode-electrolyte interface. Unfortunately, there exist other significant challenges. Dimethyl sulfoxide (DMSO) binds strongly to Mg^{2+,36} and the high desolvation energy is believed to prohibit Mg electrodeposition from DMSO containing electrolytes. Mg electrodeposition is possible from liquid sulfone based electrolytes, on the other hand, but high interfacial impedances lead to irregular Mg deposit morphologies. ^{37,38} Unlike the solid electrolyte interface (SEI) formed on the Li anode, which is Li⁺ conductive with low electronic conductivity, the SEI formed

^{*}Electrochemical Society Member.

^zE-mail: Jennifer.L.Schaefer.43@nd.edu

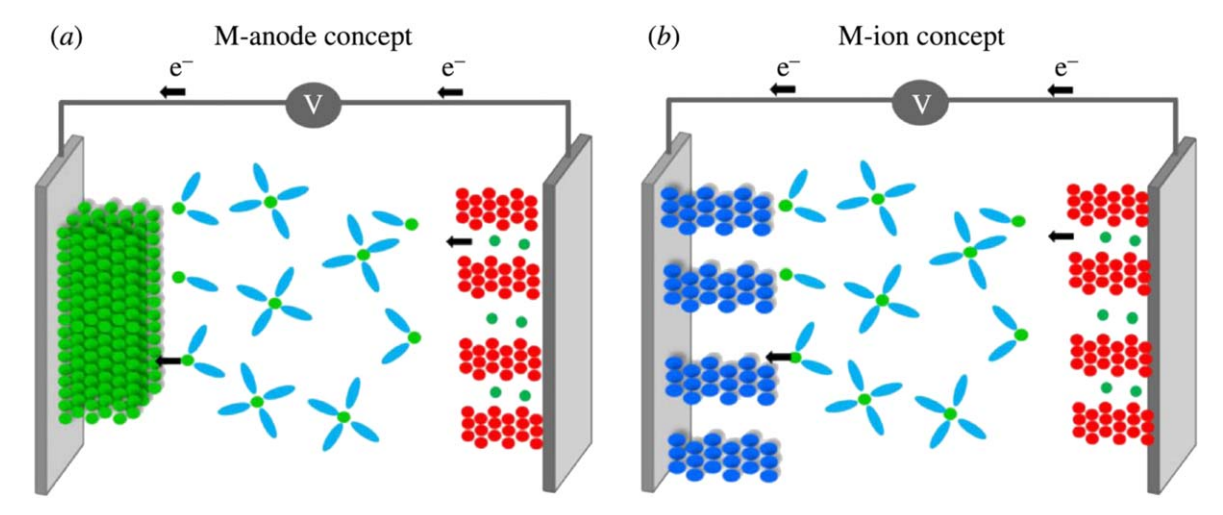


Figure 1. Schematic of a battery cell using a metal anode (a) or an insertion-type anode (b), (reprinted from Ref. 10).

in situ on the Mg anode with the large majority of electrolytes is not Mg²⁺ conductive, leading to Mg anode passivation that prevents rechargeability. In lithium ion battery systems, the cathode electrolyte interface (CEI) is also important in order to utilize various cathode materials with high operation potential (>4.5 V vs Li) with high Coulombic efficiency.³⁹ Thus, compatibility with cathode should also be considered. Incompatible solvents for bare Mg metal anodes include molecules with hydroxyls, primary and secondary amines, esters, ketones, cyanides, and thiols, such as water, alcohols, acetonitrile, dimethylformamide, and organic carbonates. Trace solvents remaining following polymer electrolyte processing as a result of incomplete drying or handling in air likely result in artificially high ionic conductivities as well as unsuitable reactivity leading to passivation of the bare Mg metal anode. Incompatible salts include those with anions typical for lithium batteries and widely available anions, such as PF₆-, BF₄-, ClO₄-, NO₃-, CH₃COO⁻, triflate (Tf⁻, SO₃CF₃⁻), and TFSI⁻ [N(SO₂CF₃)₂⁻]. It is noted that DFT calculations indicate that while bare TFSI is stable at the Mg anode at relevant potentials, the C-S bond in the MgTFSI⁺ pair is unstable under such conditions.⁴⁰ Therefore, TFSI salts should only be used with unprotected Mg metal anodes under conditions with supporting salts (i.e., $MgCl_2$, ionic liquids) such that formation of $MgTFSI^+$ is unfavorable. 41–43 Liquid magnesium electrolytes based on Grignard salts, hexamethyldisilizane (HMDS⁻) salts, borohydrides (BH₄⁻), and halide-containing salt mixtures (mixtures of MgCl₂, AlCl₃, or related, with each other or any of the aforementioned salts) are largely suitable for reversible electrochemistry against the Mg metal anode, but they suffer from other disadvantages such as low oxidative stability, intolerably high reactivity, and/or high corrosivity. Development of Mg salts with anions that are chemically and electrochemically stable against Mg metal, non-corrosive, and that have high oxidative stability is ongoing. Promising examples of such salts include magnesium tetrakis(hexafluoroisopropyloxy) borate (Mg[B(OC(H)(CF₃)₂)₄]₂),⁴ carborane clusters (Mg(CB₁₁H₁₂)₂), 45,46 and pinacolatoborate $(Mg[B(O_2C_2(CF_3)_4)_2]_2)^{47}$; these salts have been demonstrated in liquid magnesium electrolytes but not yet in polymer electrolytes.

It is noted that the very large majority of magnesium polymer electrolytes reported thus far include either solvents or salts that are not compatible with the bare Mg metal anode. Some of these studies provide insight into Mg salt complexation and transport in polymers, while others could be relevant for Mg-ion batteries or for future Mg metal batteries employing an artificial SEI at the anode. An artificial SEI is a protective, Mg²⁺ conducting thin layer that is coated on the anode prior to electrochemical cycling to act as an SEI, in order to enable utilization of a wider range of electrolyte compositions without further decomposition.

Characterization Techniques for Electrolyte property Evaluation

Ionic conductivity.—Polymer electrolytes have higher mechanical and thermal stability than liquid electrolytes. However, the ionic conductivity of polymer electrolytes is relatively low; most SPEs have conductivity less than 10^{-4} S cm⁻¹ at room temperature, which is the lower threshold considered necessary for most lithium battery applications.⁴⁹ Thus, improving ionic conductivity is important for polymer electrolytes to be practical.

Ionic conductivity can be measured via AC impedance spectroscopy with thin electrolyte films sandwiched between two non-blocking electrodes. The DC ionic conductivity, σ , is the sum of the long-range conduction from all mobile ion species in the electrolyte and can be described as:

$$\sigma = \sum_{i} n_i q_i \mu_i,$$

where n_i is the conducting ion number, q_i is the ion charge, and μ_i is the ion mobility for mobile ion species i. For monovalent cation salts, MX (e.g. M = Li), mobile ion species can be approximated as M^+ and X^- in dilute systems. For Mg salts with monovalent anions, MgX₂, mobile ion species can be fully dissociated ions, Mg²⁺ and X^- , and/or ionic complexes [i.e., MgX⁺, Mg₂X₃⁺, MgX₃⁻] over a wide range of concentration. We note that a myriad of techniques has been used to elucidate the complicated nature of speciation of ionic complexes in magnesium liquid electrolytes. ^{38,41,50–52} The implication is that a simple ionic conductivity measurement alone is not a good indicator of the adequacy of magnesium conduction, as the bulk conductivity may be dominated by anion transport.

Ionic conductivity over a given temperature range is typically presented in an Arrhenius plot (log ionic conductivity vs 1000/T), where the temperature dependence of ionic conductivity can be easily observed. In liquid, ceramic, crystalline polymer, or glassy polymer electrolytes, the typical temperature dependence of the ionic conductivity is Arrhenius in nature, shown as linear in the aforementioned plot.²⁷ In amorphous SPEs above the glass transition temperature (T_g), the temperature dependence of ionic conductivity is Vogel-Tammann-Fulcher (VTF) in nature. VTF behavior can be described as

$$\sigma = \sigma_0 \exp\left(-\frac{B}{T - T_0}\right),\,$$

where σ is the ionic conductivity, σ_0 is the pre-exponential factor and B is the pseudo-activation energy, T is the temperature, and T_0 is the Vogel temperature. VTF behavior can be observed in polymer

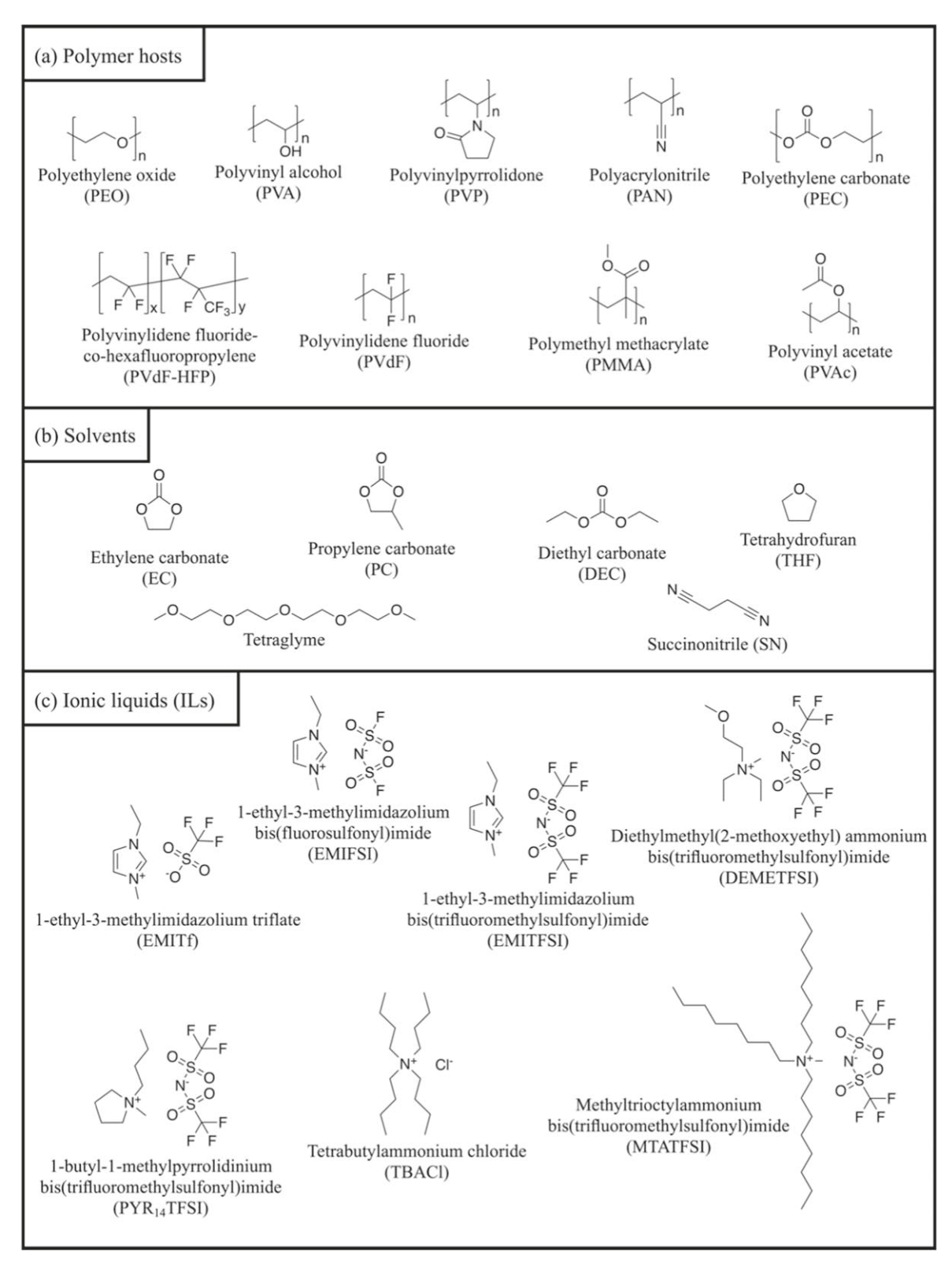


Figure 2. Molecular structures of (a) polymer hosts, (b) solvents, and (c) ionic liquids for polymer electrolytes used in the prior literature.

electrolytes where ionic conduction is coupled with polymer segmental motion. GPEs can show either Arrhenius or VTF behavior, depending on the predominant ion transport mode(s). Ion transport mechanisms in solid polymer electrolytes are well described in several recent articles.^{27,53}

Ion transference number.—For simple monovalent salt doped polymers, there is contribution from both cation and anion conduction to the total ionic conductivity. In most rechargeable battery systems, the cation conduction is of interest since the metal cation is the active ion participating in the charge/discharge reaction. In order

to consider the net charge carried by metal species, the transference number (T_+) should be determined. ^{27,54} Due to the aforementioned complexity of speciation in multivalent electrolytes, ion transference numbers are arguable both more difficult and more important to determine for magnesium polymer electrolytes than for lithium polymer electrolytes.

Several methods are reported for determination of the transference number. The most common method to estimate the transference number of a metal cation in a polymer electrolytes is the Bruce-Vincent method, wherein potentiostatic polarization is applied to a symmetric cell with non-blocking metal electrodes (the metal corresponding to the active cation species, e.g. lithium metal for Li⁺) and AC impedance measurements conducted both before and after the polarization.^{54,55} If the polarizing potential is small (~ 10 mV) and ion-ion interactions are negligible, ²⁷ the transference number can be calculated as:

$$T_{+} = \frac{i_{SS}(\Delta V - i_{SS}R_{ss})}{i_{0}(\Delta V - i_{0}R_{0})}$$

where i_{SS} and i_0 are the steady state and initial currents, R_{ss} and R_0 are steady state and initial resistances determined from impedance spectroscopy, and ΔV is the applied potential.

This method is commonly applied to characterize lithium polymer electrolytes. We note that lithium deposition/dissolution can occur with relatively small under/overpotentials. For Mg systems, however, the potential required for magnesium metal electrodeposition/dissolution is commonly hundreds of millivolts. Passivation of the Mg surface (formation of a surface layer that is not Mg²⁺ conductive) is another phenomenon that affects evaluation of the current response to polarization.

In addition to electrochemical techniques, pulsed field gradient nuclear resonance spectroscopy (PFG NMR, also referred to as diffusion NMR) is commonly used to estimate the self-diffusion coefficient of ⁷Li and/or ¹⁹F in lithium electrolytes. Then, the Nernst-Einstein equation may be applied to estimate the lithium transference number and lithium conductivity from the self-diffusion coefficients and total ionic conductivity. Building upon diffusion NMR, electrophoretic ⁷Li NMR has been applied to gain further insight into mobilities of ⁷Li-containing species. ^{56–60} Unfortunately, none of the Mg isotopes is as receptive to NMR experiments (relative receptivity of 0.000268 for ²⁵Mg, compared with 0.27 for ⁷Li and 1 for ¹H)⁶¹; thus far, there are no reports of diffusion or electrophoretic NMR on magnesium isotopes. Thus, evaluating the transference number of magnesium electrolytes is not straightforward through either electrochemical or NMR techniques.

Reversible cycling.—In addition to Mg transport, a successful polymer electrolyte must support reversible Mg redox reactions as essential for the rechargeable magnesium battery of interest. We highlight a recent review by Ponrouch and colleagues that details the difficulties and details to consider when accessing battery materials for sodium, potassium, magnesium, and calcium-based systems; propensity for side-reactions means that electrochemical cell design is particularly important. ⁶² We note that polymer electrolytes are not as easily paired with high surface area capacitive electrodes such as activated carbon cloth for fundamental testing, and that overall further advances in standardization of evaluation methods of multivalent polymer electrolytes are necessary to further this field.

Reversible Mg deposition/dissolution, required for successful pairing with Mg metal anodes, can be probed via cyclic voltammetry (CV) with asymmetric cells (i.e., Mg|Pt, Mg|Cu, Mg|SS). Equal current due to Mg deposition/dissolution, equating to 100% Coulombic efficiency and no side-reactions, is desired. Achieving high efficiency, reversible Mg deposition and dissolution with a polymer electrolyte is no small feat, and thus far there are limited successful reports. ^{63–65} Both electrodeposition and dissolution is facile for Li with most polymer electrolytes while the situation for Mg is not yet well understood. In an asymmetric cell design with a

Mg metal counter electrode as the Mg source and a metal current collector as the working electrode, the polymer electrolyte must support both electrodeposition at the working electrode and electrodissolution at the counter electrode in order to achieve substantial electrodeposition. Therefore, lack of Mg electrodissolution with a polymer electrolyte could potentially be as big or bigger of an issue than the Mg electrodeposition process. Use of alternative cell designs is necessary to probe these individual processes.

Galvanostatic charge/discharge cycling may be performed to evaluate Coulombic efficiency and the suitability of polymer electrolytes with intercalation, conversion, organic, and alloying electrodes. As noted by other recent articles, there exist very limited numbers of hosts that can reversibly intercalate and deintercalate Mg2+ without formation of side-products such as MgO and in the absence of co-intercalating solvents such as water. 66,67 In particular, MnO₂ operates as a conversion cathode rather than an intercalation cathode, with irreversible formation of MgO thermodynamically favored. V₂O₅, another popular choice, shows facile intercalation in the presence of water whereas in dry electrolytes the Mg²⁺ diffusion is too slow to allow more than surface reactions on reasonable timescales. The lack of suitable magnesium intercalation cathode materials is a challenge that polymer electrolyte researchers should be aware of. Chevrel phase Mo₆S₈, while of unpractically low operating potential, is amenable to reversible Mg²⁺ interaction and deintercalation and is therefore a suitable cathode material for new electrolyte testing. Elemental sulfur, another common electrode material for pairing with metal anodes, is also difficult to couple with Mg due to multiple challenges including the oxidation of MgS. Polymer electrolyte researchers are therefore encouraged to carefully consider conditions and cathodes for full cell testing.

Given the lack of conclusive reports of successful, long-term full cell testing with magnesium polymer electrolytes, it is worth highlighting the reports that do so with Mo $_6S_8$ cathodes. Stable galvanostatic cycling of a Mg|Mo $_6S_8$ cell was observed at 100 °C for over 150 cycles with a solid polymer electrolyte (SPE) composed of PEO-Mg(BH $_4$) $_2$ with MgO nanofiller; this is the only such successful report with a magnesium SPE. 63 Earlier, galvanostatic cycling of a Mg|Mo $_6S_8$ cell with a gel polymer electrolyte (GPE) composed of PVdF with Mg(AlCl $_2$ EtBu) $_2$ in THF showed a stable discharge capacity for 10 cycles at >60 °C. 64 Most recently, a crosslinked GPE containing Mg(BH $_4$) $_2$ -MgCl $_2$ in THF supported stable cycling of Mg|Mo $_6S_8$ for 250 cycles at room temperature. 65

Electrochemical stability.—Electrochemical stability windows are assessed via linear sweep voltammetry (LSV). Three electrode systems are preferable, however, it is difficult to make such a configuration with polymer electrolytes. Thus, two electrode (working and counter/reference) cells are often used with Mg metal as the counter/reference electrode. The Mg metal electrode can act as a quasi-reference electrode since the charge is consumed to Mg deposition/dissolution rather than potential change. The passivation of the Mg anode alters the electrode potential during the measurement. 62 Complications associated with the use of a Mg quasi-reference electrode should not be ignored. 62

NMR.— 25 Mg is quadrupolar with a spin number of 5/2 and relative receptivity of $2.68 \times 10^{-4} {}_{.61,68}$ Those characteristics of 25 Mg results in lower signal intensity and a broadened peak, which makes the analysis of 25 Mg NMR more complicated and less common. 69

Recently, ²⁵Mg solid-state NMR was performed to investigate the interaction between Mg ions and PEO. ⁶³ Pure Mg(BH₄)₂ salt showed a typical second order quadrupolar pattern, which was not found in Mg(BH₄)₂-PEO, indicating the strong interaction between Mg and PEO. Mg(TFSI)₂-PEO, where Mg²⁺ is more dissociated, showed a resonance peak, which implies interaction of Mg with coordinating six O on PEO. ²⁵Mg NMR has also been applied to liquid magnesium electrolytes. ^{70–72} Furthered use of ²⁵Mg NMR, as well as multinuclear NMR on isotopes present in the anion(s), solvent(s), and/or polymer(s), is encouraged in future polymer

electrolyte studies to provide more elucidation of ionic speciation and interactions.

Other techniques.—Common characterization methods for polymer electrolytes, including differential scanning calorimetry (DSC), X-ray diffraction (XRD), scanning electron microscopy (SEM) with energy dispersive X-ray spectroscopy (EDS), Fourier transform infrared spectroscopy (FT-IR), and others are well described in detail in a review article by Sharma and colleagues.³³ In brief, DSC is used to understand the thermal behavior of polymer electrolytes (including the glass transition and melting transition temperatures, Tg and Tm), which is crucial to understanding the temperature dependence of ionic conductivity. Further, T_m may be an indication of the temperature range where the polymer maintains dimensional stability. SEM-EDS can be used to evaluate the morphology and elemental composition of polymer films (e.g. porosity) and of electrodes after metal deposition. FT-IR and Raman spectroscopy is used to probe the ion-ion interaction and ion-polymer interaction in polymer electrolytes; these two techniques are also frequently used to understand ion complexation and speciation in liquid magnesium electrolytes. 40,53,73

Solid Polymer Electrolytes (SPEs)

PEO-based SPEs.—From the report of the first lithium conducting poly(ethylene oxide) (PEO)-based SPE, ^{76,77} plenty of PEO-based polymer electrolytes have been investigated. Due to its low glass transition temperature (ca. −60 °C) and good coordinating ability to Li⁺ which facilitates lithium salt dissociation, PEO (the short-chain version is commonly referred to as poly(ethylene glycol) (PEG)) has been widely used as a host material for lithium conducting polymer electrolytes. Thus, earlier studies on magnesium conducting SPEs introduced PEO as a host material in conjunction with magnesium analogs of common lithium salts. Ionic conductivity and characterization techniques of magnesium SPEs introduced in this review are summarized in Table I.

Magnesium conducting PEO-based SPEs, comprised of binary polymer-salt mixtures with magnesium salts (e.g. MgCl2, Mg(ClO₄)₂, Mg(SCN)₂ and Mg(CF₃SO₃)₂ (or Mg(Tf)₂)) were reported in the late 1980's in early investigations of polymer electrolytes for magnesium batteries. 78,99-101 Even though the total ionic conductivity above the melting point of PEO was close to $10^{-5}\,\mathrm{S}~\mathrm{cm}^{-1}$ for these electrolytes, the ionic conductivity at room temperature was low ($\sim 10^{-9}\,\mathrm{S}~\mathrm{cm}^{-1}$) for PEO-based electrolytes with MgCl₂ and Mg(SCN)₂ salts. Higher ionic conductivity (10⁻⁵ - $10^{-7}\,\mathrm{S\,cm}^{-1}$) was achieved at room temperature with different magnesium salts such as $\mathrm{Mg(ClO_4)_2},^{100,84}\,\mathrm{Mg(NO_3)_2},^{80}$ and Mg(TFSI)₂. ⁷⁹ However, the ion conduction in these electrolytes might be dominated by the anionic species. Negligible magnesium transport ($t_{Mg2+} < 0.005$) was observed by a magnesium transference number measurement on MgCl2 at 100 °C, using DC polarization and complex AC impedance analysis with Pt|Mg cells.⁷⁸ Shi and Vincent conducted a polarization test with PEO-Mg(Tf)₂ and suggested that the Mg ion cannot be transported efficiently via segmental motion/site percolation due to the strong electrostatic interaction of Mg²⁺ with the ether chain oxygens. ^{102,103}

In the meantime, Bakker and colleagues investigated contact ion pair (CIP) formation and cation coordination with $Mg(TFSI)_2-(PEO)_n$ using FT-IR. ⁷⁹ Ion pairs were observed with highly concentrated Mg salt (n < 9). Either the coordination number of the cation at high salt concentration (n = 9 – 12) or the lability of the cation-polymer bond at relatively low concentration (n < 16) controlled the ionic conductivity and glass transition behavior. PEO-Mg(ClO₄)₂ structure was also studied by Reddy and colleagues. ⁸⁴ Decreased crystallinity of PEO with increasing salt concentration was observed via DSC. FT-IR showed that C-O-C stretching peaks around $1000-1200 \, \mathrm{cm}^{-1}$ decreased by addition of salt, resulted from the strong interaction between Mg^{2+} cations and the ether oxygen on PEO. The ClO_4 stretching peak shifted with

coordination, resulting in two peak regions (free anion at \sim 623 cm⁻¹ and associated ClO₄⁻ at 634.5 cm⁻¹). The ionic conductivity of the electrolyte decreased when a notable associated ClO₄⁻ peak was observable, again indicating that ClO₄⁻ is the predominant mobile species.

Cyclic voltammetry results showed that reversible magnesium deposition/dissolution could not occur in either PEO-MgCl₂ or PEO-Mg(ClO₄)₂; likely high desolvation energy or lack of ionic species is the problem with PEO-MgCl₂ while Mg(ClO₄)₂ passivates the magnesium electrode surface. There had been preliminary tests of cells with PEO-Mg salt binary electrolytes in conjunction with a Mg anode and different cathode materials (e.g. TiS₂, 101 V₆O₁₃, 101 (I₂ + C + electrolyte), 80 however, reversible Mg charge/ discharge has never been confirmed with use of a pure PEO-Mg salt binary electrolyte.

In the meantime, PEO-based copolymer hosts were also studied by Acosta and colleagues, 82 who compared PEO-based electrolytes to PEO-poly(propylene oxide) (PPO) and PEO-poly(octofluoro pentoxy-trifluoro-ethoxy phosphazene) (PPz)) with Mg(Tf)2 salt. PEO-PPz electrolytes showed at least one order of magnitude higher ionic conductivity over the temperature range of 50 °C–110 °C than that of PEO and PEO-PPo electrolytes. At 50 °C, the ionic conductivity of PEO-PPz based electrolyte was $7.4\times10^{-6}\,\mathrm{S~cm^{-1}}$, whereas $3.2\times10^{-8}\,\mathrm{S~cm^{-1}}$ and $8.3\times10^{-8}\,\mathrm{S~cm^{-1}}$ were reported for PEO and PEO-PPO based electrolytes. This result was due to the plasticizing effect of PPz in the polymer matrix; transference number studies were not conducted.

Anilkumar and colleagues investigated a PEO-PVP (poly(vinyl pyrrolidone)) blend polymer electrolyte with Mg(NO₃)₂ salt. ⁸¹ It was confirmed that the salt was completely dissolved in the polymer matrix within the tested concentration range up to 30 wt%, where the optimum ionic conductivity of $5.8 \times 10^{-4} \, \mathrm{S \, cm^{-1}}$ was observed at room temperature. Cyclic voltammetry showed non-negligible redox current only at substantial potentials (inflection on the negative scan at $\sim -1.5 \, \mathrm{V \, vs \, Mg^{2+}/Mg}$), which is unsurprising as the high oxygen content of the nitrate anion renders it unstable against bare Mg metal.

In an attempt to improve ionic conductivity, ceramic fillers were introduced to magnesium polymer electrolytes. Dissanayake and colleagues reported a composite polymer electrolyte PEO-Mg(ClO₄)₂ with 10 wt% of Al₂O₃. ⁸⁵ The ionic conductivity was improved about 20 times to $\sim\!2\times10^{-6}\,\mathrm{S}\,\mathrm{cm}^{-1}$ with addition of 10 wt% Al₂O₃. The increase in conductivity was relatively large compared to the minor change in T_g of about 3 K. Thus, they concluded that the improvement of ionic conductivity was decoupled from T_g and due to surface interactions between –OH functional groups on the Al₂O₃ surface and the ClO₄ $^-$ anions.

 TiO_2 , another passive filler, was introduced into $PEG_{4000}\text{-}based$ electrolytes by Polu and colleagues, $_{85}PEG_{^-15}Mg(CH_3OO)_2$ with 0–20 wt% of titanium oxide (TiO₂). 86 The ionic conductivity increased from $10^{-6}\,\mathrm{S}\,\,\mathrm{cm}^{-1}$ to $5\,\times\,10^{-5}\,\mathrm{S}\,\mathrm{cm}^{-1}$ at $30\,^{\circ}\mathrm{C}$ with 10 wt% of TiO₂. 86,104 A primary battery discharge test on a Mg|(I₂ + C + electrolyte) cell indicated the conduction of Mg. Then they compared effect of TiO₂ or CeO₂ with $_{85}PEG_{^-15}Mg(NO_3)_2$ and both showed improved ionic conductivity, though, more improvement was realized by TiO₂ likely due to the stronger Lewis acidity of the TiO₂ surface than that of the CeO₂. 105

Effects of filler types and sizes on ion conduction were studied by Agrawal and colleagues with PEO-Mg(Tf)₂ containing SiO₂, TiO₂, MgO nano (<100 nm), and MgO micro (\sim 44 μ m) filler particles. For both ionic conductivity and magnesium transference number, TiO₂ and MgO nanofillers were superior to that of SiO₂ nanofillers and MgO microfillers, resulting in an ionic conductivity of 1.5 \times 10⁻⁵ S cm⁻¹ and transference number of 0.37. It is worth noting that there was noticeable difference when using the two different size of MgO fillers, but there was no such difference between MgO nanofillers and TiO₂ fillers.

Perhaps the most remarkable report of a Mg polymer electrolyte to date is that by Shao and colleagues of the composite solid polymer

Table I. Summary of ionic conductivity and other characterization results of reported magnesium SPEs. RT = room temperature. Bold indicates a particularly exceptional result.

Mg salt	Polymer host	Filler	Ionic conductivity (S cm ⁻¹ at RT)	T^{+}	Specific capacity (mAh g ⁻¹)	Other characterization	References
MgCl ₂	PEO	_	~10^9	_	_	_	78
MgTFSI ₂	PEO	_	$\sim \! \! 10^{-7}$		_	FT-IR	79
$Mg(NO_3)_2$	PEO	_	1.34×10^{-5}	_	_	_	80
$Mg(NO_3)_2$	PEO-PVP	_	5.8×10^{-4}	_	_	$CV (Mg MgMn_2O_4)$	81
$Mg(Tf)_2$	PEO-PPz	_	7.38×10^{-6} (50 °C)	_	_	_	82
$Mg(Tf)_2$	PEO	TiO ₂ , MgO	1.6×10^{-5}	0.37	_	_	83
Mg(ClO ₄) ₂	PEO	Al_2O_3	1.42×10^{-6}	_	_	_	84
$Mg(ClO_4)_2$	PEO	MgO	2×10^{-6}	_	_	_	85
Mg(CH ₃ COO) ₂	PEG	TiO_2	1.06×10^{-4} (30 °C)	_	_	$Discharge \; (Mg (I_2+C+electrolyte)) \\$	86
$Mg(BH_4)_2$	PEO	MgO	<u> </u>	_	$100 (Mg Mo_6S_8)$	CV (SS Mg or Mg Mo ₆ S ₈) ²⁵ Mg NMR	63
$Mg(Tf)_2$	PVA	_	5.41×10^{-4}	_	_	FT-IR AFM	87
$Mg(NO_3)_2$	PVA-PEG	_	9.63×10^{-5} (30 °C)	_	_	_	88
$Mg(NO_3)_2$	PVA	_	7.36×10^{-7} (30 °C)	_	_	DSC Dis. $(Mg (I_2 + C + electrolyte))$	89
$Mg(CH_3COO)_2$	PVA	_	1.34×10^{-7} (30 °C)	_	_	Dis. $(Mg (I_2 + C + electrolyte))$	90
$Mg(ClO_4)_2$	PVA-PVP	_	1.1×10^{-4}	_	_	FT-IR CV (Mg Mg) LSV (SS Mg, 3.5 V)	91
$Mg(ClO_4)_2$	PVA-PAN	_	2.96×10^{-4}	_	_	LSV (SS Mg, 3.65 V) Discharge (Mg MnO ₂)	92
$Mg(NO_3)_2$	PVA-PAN	_	1.71×10^{-3}	_	_	LSV (SS Mg, 3.4 V) Discharge (Mg MnO ₂)	93
Mg(TFSI) ₂			6.0×10^{-6}			DSC	94
Mg(ClO ₄) ₂	PEC	_	5.2×10^{-5} (90 °C)	_	_	LSV (SS Mg, Mg(TFSI) ₂ , ~2.2 V)	
$Mg(TFSI)_2 + LiFSI$	PEC	_	1.0×10^{-5} (80 °C)	_	_	FT-IR CV (Mg Mg) SEM-EDX on deposit	95
Mg(Tf) ₂	PVdF-HFP	_	$\sim 10^{-3}$	_	_		96
$Mg(ClO_4)_2$	PVdF-HFP/ PVAc	_	1.60×10^{-5}	_	_	LSV (SS Mg, 3.5 V)	97
$Mg(NO_3)_2$	PVdF	MgO	(30 °C) 1.04 × 10 ⁻⁴	_	_	XRD DSC	98

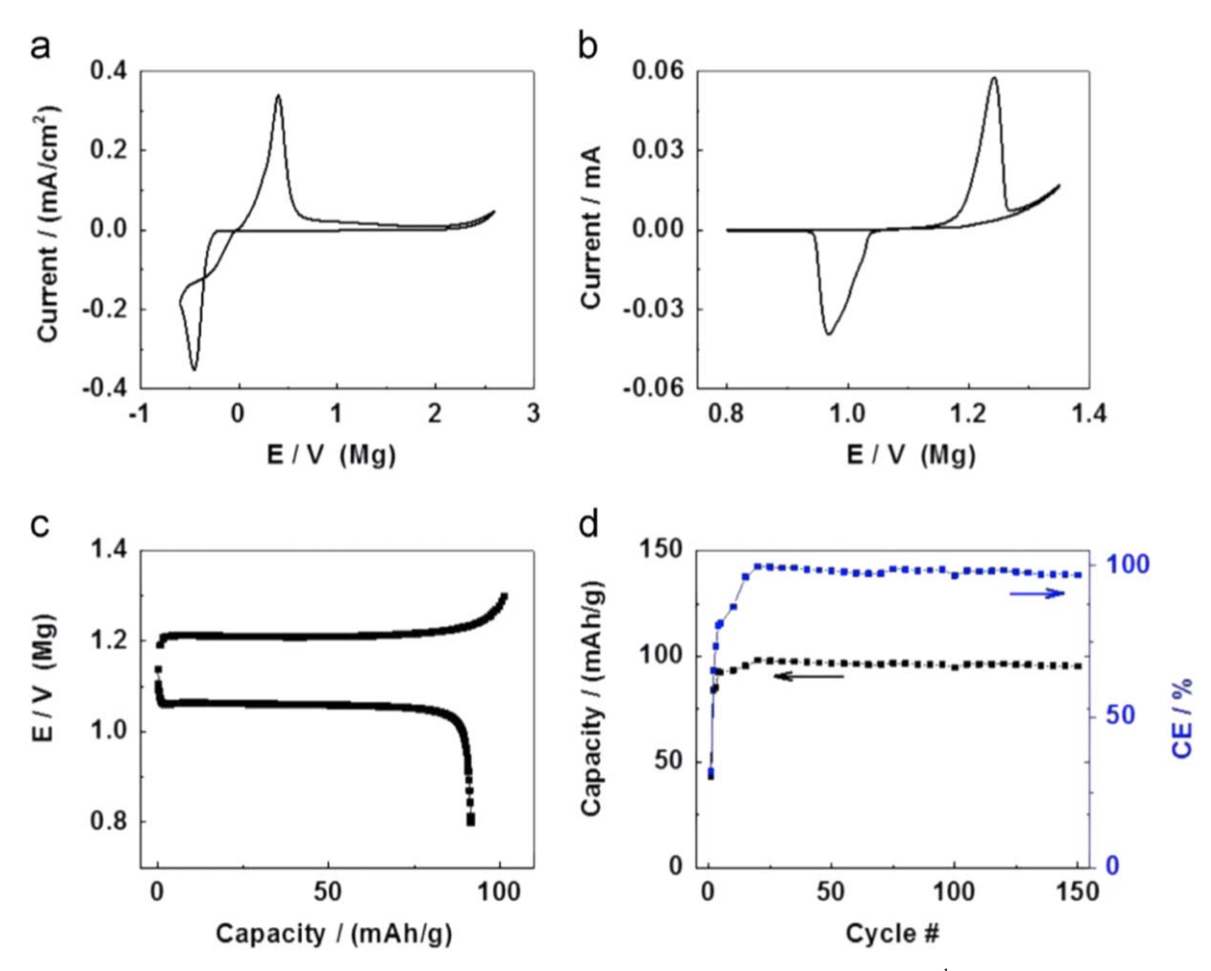


Figure 3. Electrochemical performance of the nanocomposite electrolyte $Mg(BH_4)_2$ –MgO–PEO. (a) CV (20 mV s⁻¹) of Mg plating/ stripping on a stainless steel electrode. (b) CV (0.05 mV s⁻¹) of Mg intercalation/deintercalation in Mo_6S_8 . (c) Discharge/charge curve. (d) Cycling stability of a solid-state Mg cell. All electrochemical tests were done in coin cells at 100 °C. Cell architecture: (a) SS/Mg(BH₄)₂–MgO–PEO/Mg, (b)–(d) Mo_6S_8 /Mg(BH₄)₂–MgO–PEO/Mg. (Reprinted from Ref. 63).

electrolyte PEO-Mg(BH₄)₂ with MgO nanofiller. ⁶³ Electrochemical performance results are shown in Fig. 3. They showed reversible magnesium electrodeposition and dissolution at low under/over-potentials and stable galvanostatic cycling with Mg[Mo₆S₈ cells more than 150 cycles with a Coulombic efficiency of about 98% without capacity loss at 100 °C. With PEO-Mg(TFSI)₂, the authors report that no reversible electrochemistry is observed via CV, perhaps due to the strong coordination between fully dissociated Mg²⁺ and the oxygens on the PEO chains. With detailed ²⁵Mg-NMR and simulation studies, the authors concluded that the reversibility supported by Mg(BH₄)₂-PEO-MgO might be due to the formation of solvated [MgBH₄]⁺ ions. Unfortunately, the low oxidative stability of the borohydride anion (1.7 V vs Mg²⁺/Mg)¹⁰⁶ limits its practicality.

PVA-based SPEs.—Due to the hydrogen bonding of the hydroxyl side groups, poly(vinyl alcohol) has a relatively high glass transition temperature (85 °C) and melting temperature (\sim 160 °C), compared to PEO. With the higher melting temperature, PVA homopolymer can be self-supporting over a higher temperature range. We note that the high density of hydroxyl groups on PVA likely makes this polymer unsuitable for use with unprotected Mg metal anodes.

The temperature dependence of ionic conductivity in PVA-based electrolytes follows Arrhenius behavior. It is found that the ion conduction is decoupled from polymer segmental motion for lithium PVA electrolytes. ¹⁰⁷ A similar result was also found for

Mg-conducting PVA electrolytes,⁸⁷ suggesting that the ion conduction occurs through ion hopping between ion aggregates rather than segmental motion of the polymer host.

Ionic conductivity can be improved by softening the host materials by using polymer blends. Polu and colleagues blended PEG₄₀₀₀ into PVA. The PVA-PEG (1:1)-Mg(NO₃)₂ electrolyte displayed two orders of magnitude higher ionic conductivity at 30 °C ($\sim 10^{-5} \, \mathrm{S \, cm^{-1}}$) compared with the PVA homopolymer electrolyte. ⁸⁸ Similarly, for the PVA-PVP (1:1) blend, the ionic conductivity of $\sim 10^{-4} \, \mathrm{S \, cm^{-1}}$ at room temperature was achieved with Mg(ClO₄)₂. ⁹¹ FT-IR studies showed that the inter- and intramolecular interaction between functional groups from both polymers facilitated ion conduction by formation of ion conduction pathways. Though Tg increased with salt concentration due to the electrostatic crosslinking effect of Mg²⁺, the total ionic conductivity increased, which implies ionic conduction is decoupled from segmental motion. Cyclic voltammetry was conducted on symmetric Mg|Mg cells containing PVA-PVP (1:1) - 25 mol% Mg(ClO₄)₂, however, the significant potentials required to achieve redox peaks and lack of further testing make it unclear if any of the observed current is due to the desired Mg electrochemistry or if it is entirely from side-reactions. Both PVA and ClO₄⁻ are anticipated to be reactive and cause passivation of Mg metal.

A similar result was also observed in a blend polymer host with a small amount of PAN, PVA:PAN (92.5:7.5). The ion conduction was proposed to occur via ion hopping between the coordination sites comprised of OH, C=O and C \equiv N on the polymer chains, and high total ionic conductivity up to $2.96 \times 10^{-4} \, \mathrm{S \, cm^{-1}}$ and

 $1.71\times10^{-3}\,\mathrm{S\,cm}^{-1}$ at room temperature was achieved with Mg(ClO₄)₂ and Mg(NO₃)₂ salts, respectively. 92,93 By primary battery discharge tests using Mg|MnO₂ cells, it was suggested that Mg $^{2+}$ was the mobile species which participated in the discharge reaction, but XRD was not used to confirm Mg $^{2+}$ intercalation or formation of MgO due to conversion.

PEC-based SPEs.—Aziz and colleagues introduced PEC-based magnesium conducting polymer electrolytes with Mg(TFSI)2 and Mg(ClO₄)₂ as magnesium salts up to 50 mol%. ⁹⁴ They found via FT-IR that almost 100% of TFSI ions exist in the form of free ions up to 30 mol% salt, which decreased to 90% with additional salt. Reduction/oxidation peaks were observed via CV at elevated potentials that decayed over time, likely due to Mg passivation, for Mg|Mg cells with PEC-Mg(TFSI)2, while no redox peaks were observed with PEC-Mg(ClO₄)₂. Later, the authors introduced a small amount of lithium bis(fluorosulfonyl)imide (LiFSI) salt (0.5-2.0 wt%) into PEC-40 mol% Mg(TFSI)₂ electrolyte in order to improve the ionic conductivity. The ionic conductivity at 80 °C increased about 5 times to 1.0×10^{-5} S cm⁻¹ without significant decrease of the oxidative stability. Even though the presence of Mg was confirmed via SEM-EDX in the deposit following cyclic voltammetry, neither the ratio of Li:Mg nor diffraction was reported so the efficacy of the Mg deposition is unclear.

PVdF-HFP-based SPEs.—Ramesh and colleagues reported poly (vinylidenefluoride-hexafluoropropylene) [P(VdF-HFP)]-based Mg conducting polymer electrolytes with 5–40 wt% of Mg(Tf)₂. ⁹⁶ The ionic conductivity increased with salt concentration, and the maximum ionic conductivity was observed as $\sim 10^{-3}$ S cm⁻¹ with 40 wt% salt at room temperature. It is possible that this high ionic conductivity may be due to residual solvent, as the reported drying procedure was room temperature drying without vacuum.

Later, Ponmani and colleagues investigated copolymer hosts comprised of PVdF-HFP/poly(vinyl acetate) (PVAc) and Mg(ClO₄)₂. The maximum ionic conductivity was observed with 8 wt% of salt as 1.6×10^{-5} S cm⁻¹ at 30 °C. TGA showed thermal stability up to 200 °C, where weight loss of about 20% occurs due to the acetate side chain decomposition. They suggested the electrochemical window of 3.5 V via LSV with SS|Mg cell and reversible Mg redox reaction over -4 to 4 V with Mg|Mg cells. However, the decomposition current arises from 2 V with LSV, and thus the reversible redox current observed in CV could be due to electrolyte decomposition products.

A recent study showed improvement in ionic conductivity with MgO by Nidhi and colleagues for PVdF-Mg(NO₃)₂ based electrolytes with 0–4 wt% MgO. ⁹⁸ The optimum ionic conductivity was observed as $\sim 2 \times 10^{-6}$ S cm⁻¹ with 3 wt% MgO at 40 °C, which

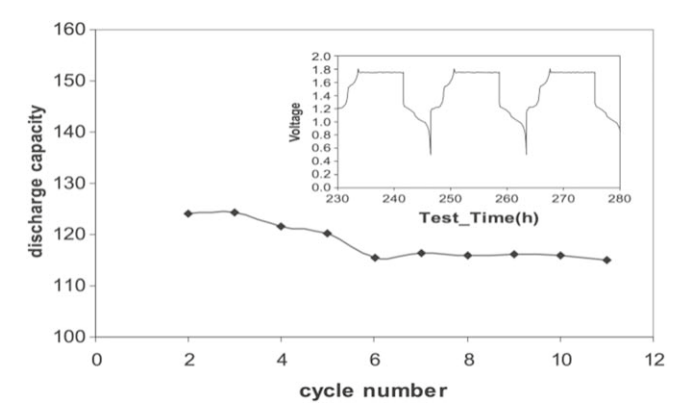


Figure 4. A typical specific discharge capacity vs cycle number plot for rechargeable magnesium battery with PVdF/Mg(AlCl₂EtBu)₂/tetraglyme gel electrolyte, Mo_6S_8 cathode, and AZ-31 magnesium alloy (3% Al and 1% Zn) as the anode material. The inset is a voltage-time curve (a chronopotentiogram) for the same battery. (Reprinted from Ref. 64).

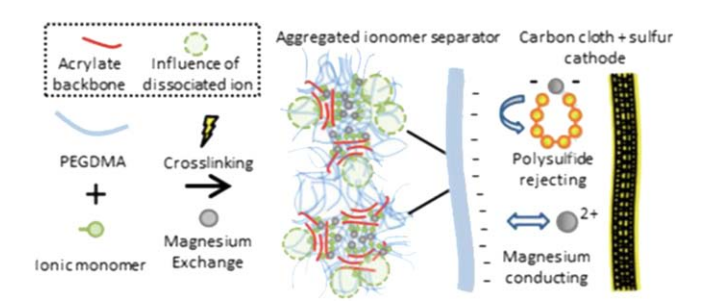


Figure 5. Schematic image of polysulfide rejection of the PEGDA-STFSIMg GPE. (Reprinted (adapted) with permission from Ref. 113 Copyright (2018) American Chemical Society.).

was about 2 orders of magnitude improved from PVdF-Mg(NO₃)₂ ($6 \times 10^{-8} \, \text{S cm}^{-1}$), by significantly decreased degree of crystallinity and crystallite size.

Liquid Crystalline Polymer Electrolytes

Dias and colleagues reported on magnesium conducting, solvent-free liquid crystalline polymer electrolytes, poly[tetraoxyethyleneoxymethylene (5-hexadecyloxy-1,3-phenylene) methylene] ($C_{16}O_5$) and similar, with different lengths of ether chains and alkyl chains. 108,109 The ionic conductivity was $2.5\times10^{-8}~S~cm^{-1}$ at 20~C and rose to $10^{-5}~S~cm^{-1}$ at 100~C. A steep ionic conductivity increase was observed around 50 °C, slightly above the temperature where the crystal to smectic liquid crystal phase transition occurred at 42~C-44~C. The authors suggested that ion conduction occurred through the two-dimensional helical polyether backbone layers which are separated by hydrocarbon layers. The authors focused on structural analysis (SAXS, XRD, SEM) and DSC, and there is no further reported electrochemical testing.

Gel Polymer Electrolytes (GPEs)

Low molecular weight ethers.—After successful Mg deposition/ dissolution was demonstrated using Grignard reagent in ethereal solvents, Liebenow reported on a PEO-based electrolyte containing Grignard reagent EtMgBr in THF, dibutyl ether, or diethyl ether. They demonstrated reversible Mg deposition/dissolution in the THF containing gel polymer electrolyte with Ni|Mg cells via CV and an ionic conductivity of 10^{-4} S cm⁻¹ at 40 °C. Aurbach and colleagues demonstrated a liquid Mg electrolyte of organohaloaluminate salt Mg(AlCl₂EtBu)₂ in THF and showed Coulombic efficiency of close to 100%. They prepared GPEs with this liquid electrolyte in polymer hosts including PEO or PVdF.⁶⁴ Reversible Mg deposition/dissolution was shown with an electrochemical stability window of 2.2 V. Galvanostatic cycling of a Mg|Mo₆S₈ cell resulted in a stable discharge capacity of \sim 110 mAh g⁻¹ for 10 cycles at >60 °C, as shown in Fig. 4. Due to the strong reducing nature of the Grignard reagents, however, neither of these electrolytes is compatible with common metal current collectors.

GPEs comprised of poly(ethylene glycol) diacrylate (PEGDA) or dimethacrylate (PEGDMA) and STFSI or 4-vinylbenzenesulfonate (SS) were investigated to reduce polysulfide shuttle effect in Mg|S batteries (Fig. 5). ¹¹³ The optimum ionic conductivity was observed as $10^{-4} - 10^{-5}$ S cm⁻¹ with PEGDA-STFSIMg swelled in Mg|S compatible liquid electrolyte (Mg(TFSI)₂-MgCl₂ in 1,2-dimethoxyethane (DME)). The ionic conductivity was higher with -STFSI and a lower concentration of ionic monomer units due to the higher dissociation. H-type cell diffusion tests and galvanostatic cycling tests on Mg|S cells showed mitigated polysulfide shuttle effect, relative to use of a liquid electrolyte with a glass fiber separator, and charging to the desired cut-off potential.

Recently, a polytetrahydrofuran (PTHF) based GPE containing Mg(BH₄)₂-MgCl₂ in THF was reported. ⁶⁵ Ionic conductivity at room temperature of $4.76 \times 10^{-4} \, \mathrm{S \ cm^{-1}}$, high Mg transference number

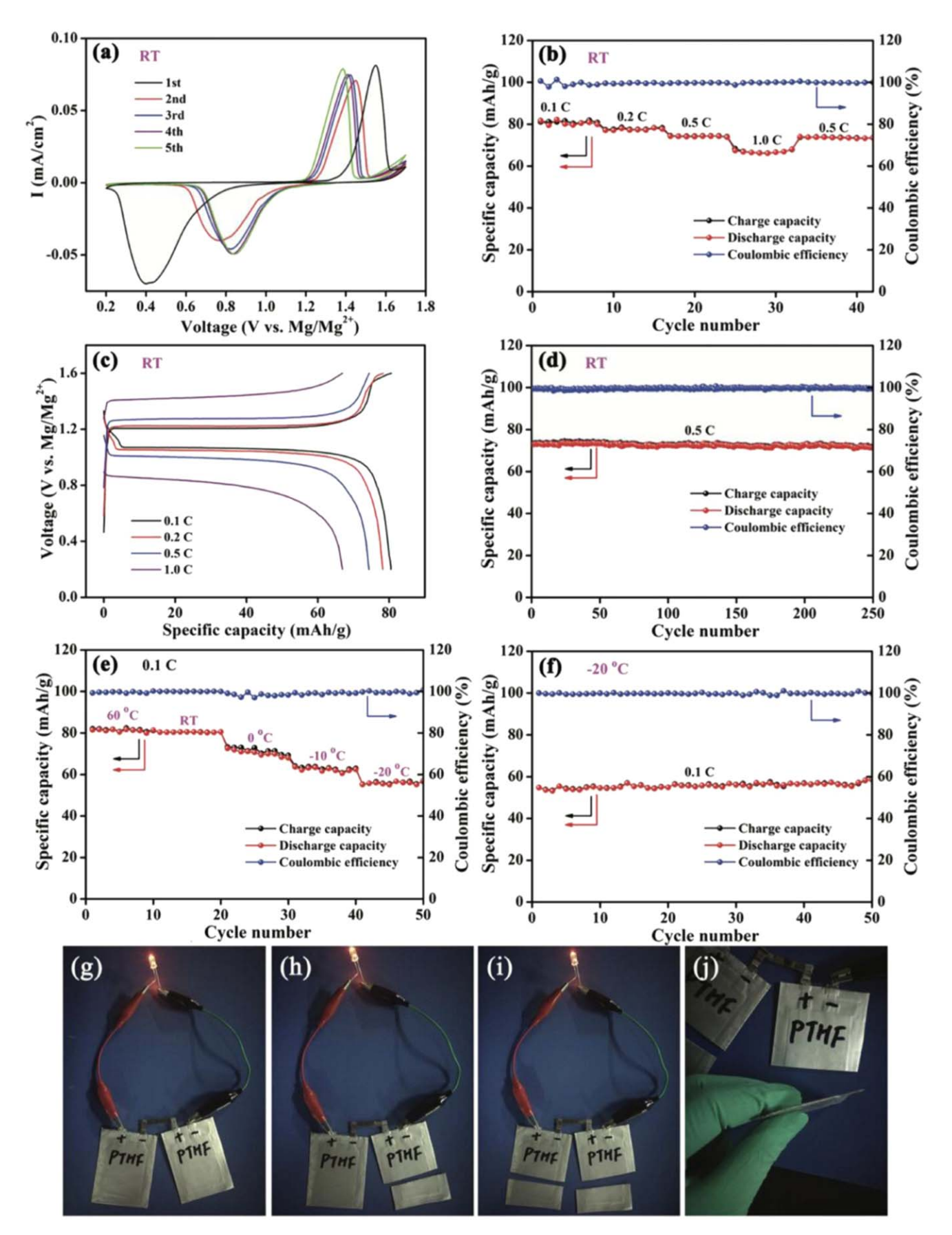


Figure 6. (a)–(f) Electrochemical characterization of the $Mo_6S_8|PTB@GF-GPE|Mg$ batteries at room temperature (RT) (a)–(d) and low temperature (e), (f): (a) the CV curves at a scan rate of $0.05~mV~s^{-1}$, (b) the specific capacity at different charge—discharge C-rate, (c) the galvanostatic charge—discharge profiles at different C-rate, (d) the cyclic stability at 0.5~C, (e) the specific capacity at 0.1~C at varied temperatures, (f) the cyclic stability at 0.1~C and at $-20~^{\circ}C$. (g)–(j) Illustration of soft-package $Mo_6S_8|PTB@GF-GPEs|Mg$ batteries under cutting test conditions. (Reprinted from Ref. 65).

(0.73), reversible Mg deposition/dissolution, and remarkable cycle retention of over 250 cycles with Coulombic efficiency of $\sim\!100\%$ at room temperature was observed with a Mg|Mo₆S₈ cell (Fig. 6). Stable cycle retention and high Coulombic efficiency for over 50 cycles was also achieved at the low temperature of -20 °C, where the ionic conductivity of the GPE was 5 \times 10 $^{-5}$ S cm $^{-1}$; this positive result is most likely due to the high transference number of the GPE. The reported results of magnesium GPEs containing low molecular weight ethers are summarized in Table II.

Higher molecular weight ethers.—Oligomeric dimethoxy-terminated poly(ethylene glycol), also called glymes, are widely used as polymer electrolyte plasticizers. Studies on the relation between Mg cation transport and molecular weight of PEG/PEO suggested that the Mg ion transport was dominated by two different mechanisms with different molecular weight. Above the critical molecular weight (3200 g mol⁻¹), the ionic conduction relies on the segmental motion/site percolation, which is not favorable for Mg²⁺ in PEO due to strong Mg-O interactions as discussed in the previous section. Under the critical molecular weight, the magnesium ion transport is dominated by vehicular diffusion of chain coordinated Mg cations, as confirmed by a polarization test with a Mg|Mg cell. 103 Both Di Noto and colleagues as well as Saito and colleagues have investigated magnesium electrolytes based on oligomeric PEG; these studies will not be discussed further here as these electrolytes are liquids rather than polymers. We also note that in many studies hydroxyl-terminated PEG is employed, which is reactive with bare Mg metal and may have somewhat different interactions with ions than methoxy-terminated PEG. 114-118

Organic carbonates.—Meanwhile, cyclic organic carbonate solvents EC and PC were considered as solvents for magnesium gel polymer electrolytes due to the high dielectric constant and boiling point, beneficial for salt dissociation and thermal stability. In liquid electrolytes for lithium-ion batteries, usually a high thermal stability solvent (EC) and low viscosity solvent, such as DMC or DEC, are used as co-solvents in order to achieve both ion pair dissociation and low viscosity. Similar approaches were also reported for Mg conducting GPEs. The ionic conductivity of gel polymer electrolytes based on organic carbonates is generally above 10⁻⁴ S cm⁻¹; results are summarized in Table III. However, the major disadvantage of this class of electrolytes is the reactivity with bare Mg. Magnesium gel polymer electrolytes containing organic carbonates will require a protected Mg anode, likely produced via adoption of an artificial SEI, to enable adequate stability and reversibility for Mg metal anode batteries, or adoption of an alternative anode.

Kumar and colleagues firstly introduced EC/PC (1/1 volume ratio) mixture as a plasticizer and Mg(Tf)₂ salt into various polymer hosts such as PAN, ^{120–122} PEO, ¹²³ PVdF, ¹²⁴ and PMMA. ¹²⁵ They showed moderate ionic conductivities of above 10⁻⁴ S cm⁻¹. FT-IR study on PEO-based GPE showed that Mg²⁺ was coordinated with PEO rather than EC/PC, even though the ionic conductivity was improved by three orders of magnitude from without plasticizers. Galvanostatic cycling was performed with PAN-, PVdF-, and

PMMA-based GPEs and showed limited cycle numbers due to the progressive passivation of the Mg|GPE interface from continuous consumption of liquid components and poor rechargeability of the MnO_2 electrodes. 121,122,125

Yoshimoto and colleagues prepared GPE mixtures of EC/DEC as plasticizers with PEO-PMA and Mg(TFSI)₂. ¹³³ Mg conduction and reversible Mg deposition/dissolution were probed via galvanostatic cycling of Mg|V₂O₅ and Mg|MnO₂.

Asmara and colleagues investigated PMMA-Mg(Tf)₂ with a plasticizer EC/DEC. ¹³⁴ The Mg transference number of 0.37 was reported, along with an electrochemical stability window of 2.42 V with the SS|Mg configuration. FT-IR showed larger portion of free ions and smaller portion of ion aggregation due to the ion dissociation by PMMA.

A PVdF-HFP based GPE with EC/DEC and Mg(Tf)₂ was demonstrated by Perera and colleagues, ¹³⁵ showing an electrochemical stability window of 2.75 V with a SS|Mg cell. The ionic conductivity was comparable to previously reported ionic conductivity of similar GPEs with organic carbonates, PVdF-EC/PC-Mg(Tf)₂ ¹²⁴ and PVdF-HFP-PC-Mg(ClO₄)₂. ¹³⁶

Addition of SiO₂ filler into PVdF-HFP EC/PC-Mg(ClO₄)₂ was considered by Oh and colleagues. ¹²⁷ Though they tried galvanostatic cycling with Mg|V₂O₅ cells, poor cycling performance was observed (\sim 50 mAh g⁻¹) due to the interfacial resistance of Mg and slow diffusion of Mg²⁺ in V₂O₅.

Later, Pandey and colleagues investigated MgO (two sizes, micro (${\sim}44~\mu m)$ and nano (${<}100~nm)$ particles) and SiO $_2$ (${\sim}7~nm)$ in composite gel polymer electrolytes composed of PVdF-HFP, EC/PC, and Mg(ClO $_2$). $^{128-131}$ Significant improvement was observed on both transference number (0.22 \rightarrow 0.4) and cyclic voltammetry peak currents for the Mg|Mg configuration with MgO, regardless of the particle size. Improvement with SiO $_2$ was smaller than that of with MgO, resulting in a cation transference number of 0.3 and smaller currents during voltammetry. The authors suggested that the improvement in Mg conduction with MgO was due to the interaction between MgO and Mg $^{2+}$. Galvanostatic cycling of Mg-MWCNT|V $_2$ O $_5$ showed a discharge capacity of 150 mAh g $^{-1}$ (V $_2$ O $_5$) for 10 cycles, however, we note that other literature suggests that intercalation of bare Mg $^{2+}$ into bulk V $_2$ O $_5$ is not sufficiently fast for this response.

Other types of nanofillers, Al_2O_3 and $MgAl_2O_4$, in PVdF-HFP with EC/PC and $Mg(Tf)_2$ gel polymer electrolyte was compared by Sharma and colleagues. Noticeable improvement in transference number was observed, with reported values of 0.66 and 0.52 for $MgAl_2O_4$ and Al_2O_3 containing electrolytes, respectively. Both fillers improved mechanical strength and porosity of the gel polymer electrolyte. Meanwhile, Tripathi and colleagues observed ionic conductivity of $5.0 \times 10^{-3} \, \mathrm{S \, cm^{-1}}$ in GPE composed of 15 wt% of PVdF-HFP and $Mg(ClO_4)_2/PC$, slightly higher than that of liquid electrolyte $Mg(ClO_4)_2/PC$ (3.63 \times 10⁻³ S cm⁻¹). Addition of Al_2O_3 filler into this GPE showed minor change in ionic conductivity while transference numbers were not reported. 137

Succinonitrile.—With high melting point $(57 \,^{\circ}\text{C})$ and dielectric constant (~ 55) , plastic crystal succinonitrile (SN) was considered as

Table II. Summary of magnesium GPEs containing low molecular weight ethers. Bold indicates reports with particularly exceptional cycling results.

Salt	Polymer host	Solvent	Ionic conductivity (S cm ⁻¹)	Charge/discharge (or CV) test configura- tion	References
EtMgBr	PEO	THF,	10 ⁻⁴ at 40 °C	(Ni Mg)	110, 111
		DBE			
$Mg(AlCl_2EtBu)_2$	PEO, PVdF	THF	$\sim 3 \times 10^{-3} \text{ (PVdF)}$	$Mg Mo_6S_8$	64
Mg(TFSI) ₂ -MgCl ₂	PEGDA-	DME	$10^{-4} - 10^{-5}$	Mg S	113
	STFSIMg				
$Mg(BH_4)_2$ - $MgCl_2$	PTHF	THF	4.76×10^{-4}	$Mg Mo_6S_8$	65

Table III. Summary of magnesium GPEs containing organic carbonates.

Salt	Polymer host	Solvent	Filler	T_{+}	Charge/discharge (or CV) test configuration	References
Mg(Tf) ₂	PAN, PEO, PVdF, PMMA	EC/PC	_	$\sim 0.37^{119}$	$Mg MnO_2$	119–125
$Mg(ClO_4)_2$	PAN	EC/PC	_	_	_	126
$Mg(ClO_4)_2$	PVdF-HFP	EC/PC	SiO_2	_	$Mg V_2O_5$	127
$Mg(ClO_4)_2$	PVdF-HFP	EC/PC	MgO	~ 0.4	(Mg Mg)	128-131
			SiO_2	\sim 0.3	Mg-MWCNT V ₂ O ₅	
$Mg(Tf)_2$	PVdF-HFP	EC/PC	Al_2O_3	0.52	_	132
υ· /-			$MgAl_2O_4$	0.66		
Mg(TFSI) ₂	PEO-PMA	EC/	_	_	$Mg V_2O_5$	133
S(/2		DEC			01 2 3	
					$Mg MnO_2$	
$Mg(TF)_2$	PMMA	EC/	_	0.37	_	134
J. 72		DEC				

a plasticizer for magnesium GPEs in order to achieve both high ion dissociation and mechanical stability at ambient temperature. Like organic carbonates, SN is chemically reactive with Mg metal. The first use of SN in Mg-conducting GPEs was reported by Sharma and colleagues with PEO-Mg(Tf)₂. ¹³⁸ The ionic conductivity was well above 10^{-4} S cm⁻¹ and this GPE showed high thermal and electrochemical stability, with a minor weight loss (~5 wt%) at 100 °C detected via thermal gravimetric analysis (TGA) and an electrochemical stability window of ~4.1 V with a SS|Mg cell. Mg conduction was suggested from a polarization test, and increased currents were present with CV of a Mg|Mg cell compared to a SS|SS cell. They suggested that Mg ion transport occurred due to the enhanced salt dissociation in the PEO-SN matrix due to higher dielectric constant than pure PEO. Sheha and colleagues also demonstrated a GPE complex with moderate ionic conductivity above 10⁻⁴ S cm⁻¹ using PVA/poly(3,4-etylenedioxythiophene): poly(styrenesulphonate) (PEDOT:PSS)-based GPE with MgBr₂ and SN as a plasticizer. Mg ion conduction was observed from the transference number of 0.28 and stable, low capacity charge/ discharge cycling of a Mg|V₂O₅ cell over 40 cycles. The electrodes were not fully utilized with SEM-EDS showing minimal change in Mg content $(0.93 \rightarrow 2.55 \text{ wt\%})$ in the cathode after discharge.

Recently, Hambali and colleagues reported a GPE of poly (vinylidene chloride-co-acrylonitrile) (PVdC-co-AN)-Mg(Tf)₂ with SN. ¹⁴⁰ Despite its low ionic conductivity (>10⁻⁶ S cm⁻¹) at room temperature, a Mg transference number of 0.33 was observed. An FT-IR study showed that both ion pairs and ion aggregates decreased with SN addition. ¹³⁸ Then, they further investigated GPEs with the same polymer host with mixed plasticizer SN/EC and two salts, Mg(Tf)₂ and Mg(TFSI)₂. ¹⁴¹ The ionic conductivity was not much improved, however, the transference number significantly increased to larger than 0.5 for both GPEs, which implies that more than half of ion conduction was Mg cations. Galvanostatic cycling of Mg|MgMn₂O₄ showed initial discharge capacities of 223 mAh g⁻¹ and 51 mAh g⁻¹ for Mg(TFSI)₂ and Mg(Tf)₂ based GPEs, respectively. Capacity decreased significantly decreased over 10 cycles, likely limited by the Mg anode passivation and cathode instability.

Ionic liquids.—Instead of organic solvents, ionic liquids (ILs) are considered as the liquid media for GPEs due to their thermal and electrochemical stability. 142-144 Ionic conductivity of the IL containing GPEs will not be discussed in detail since most of the reported values are above 10⁻⁴ S cm⁻¹ due to the intrinsic high ionic conductivity of ILs. For these systems, transference numbers are more important. Most of the reports reviewed here used 1-ethyl-3-methylimidazolium bis(trifluoromethylsulfonyl)imide (EMITFSI) or 1-ethyl-3-methylimidazolium triflate (EMITf) as the IL. It is noted that GPEs containing EMITf are expected to be reactive with bare Mg, GPEs with EMITFSI are also expected to be reactive with Mg,

unless all of the TFSI⁻ is uncoordinated with Mg²⁺ (no MgTFSI⁺). Results of IL containing Mg GPEs are summarized in Table IV.

The first Mg conducting GPE with an IL plasticizer was reported by Yoshimoto and colleagues. ^{145,146} They investigated a GPE comprised of PEO-PMA and Mg(TFSI)₂ with plasticizers EMITFSI or diethylmethyl(2-methoxyethyl) ammonium bis(trifluoromethylsulfonyl)imide (DEMETFSI). Mg transport in the GPE was proven by the DC polarization experiments by comparing steady state currents achieved with blocking electrodes (Pt) vs non-blocking electrodes (Mg). Thermal stability of the GPE with EMITFSI was confirmed via DSC, shown as a flat scan without significant decomposition/evaporation peak(s) up to 300 °C. ¹⁴⁶

Pandey and colleagues reported a GPE of PVdF-HFP-Mg(Tf)₂ with EMITf.¹⁴⁷ Mg ion conduction was confirmed via a Mg transference number measurement (0.26), and cyclic voltammetry of Mg|Mg cells resulted in redox peaks around −1.8 V and 1.5 V, respectively, with more than 4 times higher current for the former peak, obtained in the first pass (Fig. 7). TGA and LSV with SS|Mg cells indicated that the GPE was both thermally (single phase behavior within 110 °C) and oxidatively (~3.5 V) stable. Song and colleagues further investigated this GPE and reported a tensile strength test.¹⁴⁸ Even though the Young's modulus and yield strength was about 1/3 of pure PVdF-HFP for GPEs, it was still high enough for application.

Sharma and colleagues introduced SN into a PVdF-HFP based GPE with EMITf and Mg(Tf)₂. ¹⁴⁹ Galvanostatic cycling of a Mg|MnO₂ cell containing this GPE was performed, and the discharge capacity decreased significantly over 8 cycles from 40 to 5 mAh g⁻¹ as may be expected. Similarly, GPE PVA-Mg(Tf)₂ with EMITf was reported by Song and colleagues, ¹⁵⁰ and a PVdF-based GPE with tetraglyme, tetrabutylammonium chloride (TBACl), and Mg(Tf)₂ was investigated by Aravindan and colleagues. ¹⁵¹ And, Ponmani and colleagues reported a GPE composed of polymer blend PVdF-HFP/poly(vinyl acetate) (PVAc) with Mg(ClO₄)₂ and EMITf with an ionic conductivity of $\sim 10^{-3}$ S cm⁻¹ and transference number of 0.33. ¹⁵²

PEO-Mg(Tf)₂ was also investigated as a GPE with addition of EMITf 154,153 or 1-butyl-1-methylpyrrolidinium bis(trifluoromethanesulfonyl)imide (PYR₁₄TFSI). 155 Mg $^{2+}$ conduction was observed via Mg $^{2+}$ transference number testing (>0.40), and cyclic voltammetry of a Mg|Mg cell resulted in peak overpotentials at $\sim \pm 2$ V and substantially increased currents relative to the SS|SS case. A galvanostatic cycling test on Mg|TiO₂ with PEO-Mg(Tf)₂-PYR₁₄TFSI indicated the possibility of reversible charge/discharge for 5 cycles at a very slow rate of 0.015 C. FT-IR, Raman, and DSC indicated that the organic cation interacted with oxygen on the PEO chain, competing with Mg $^{2+}$, which may assist the magnesium transport. 154

Song and colleagues introduced SiO₂ filler into PEO-Mg(ClO₄)₂ with EMIFSI. 156 The ionic conductivity was 5.4×10^{-4} S cm⁻¹,

Table IV. Summary of magnesium GPEs containing ILs.							
Salt	Polymer host	Ionic liquid	Solvent (or filler)	T_{+}	Charge/discharge (or CV) test configuration	References	
				_		145, 146	
$Mg(TFSI)_2$	PEO-PMA	EMITFSI, DEMETFSI	_	(Pt Mg pol. test)	_		
$Mg(Tf)_2$	PVdF-HFP	EMITf	_	0.26^{147}	$(Mg Mg)^{147}$	147, 148	
$Mg(Tf)_2$	PVdF-HFP	EMITf	SN	_	$Mg MnO_2$	149	
$Mg(Tf)_2$	PVA	EMITf	_	_	_	150	
$Mg(Tf)_2$	PVdF-HFP	TBACl	tetraglyme	_	_	151	
$Mg(ClO_4)_2$	PVdF-HFP/ PVAc	EMITf	_	0.33	(Mg Mg)	152	
$Mg(Tf)_2$	PEO	EMITf	_	$\sim 0.45^{153}$	$(Mg Mg)^{153}$	153, 154	
$Mg(Tf)_2$	PEO	PYR ₁₄ TFSI	_	>0.40	$(Mg Mg)$ $Mg TiO_2$	155	
$Mg(ClO_4)_2$	PEO	EMIFSI	(SiO_2)	_	_	156	

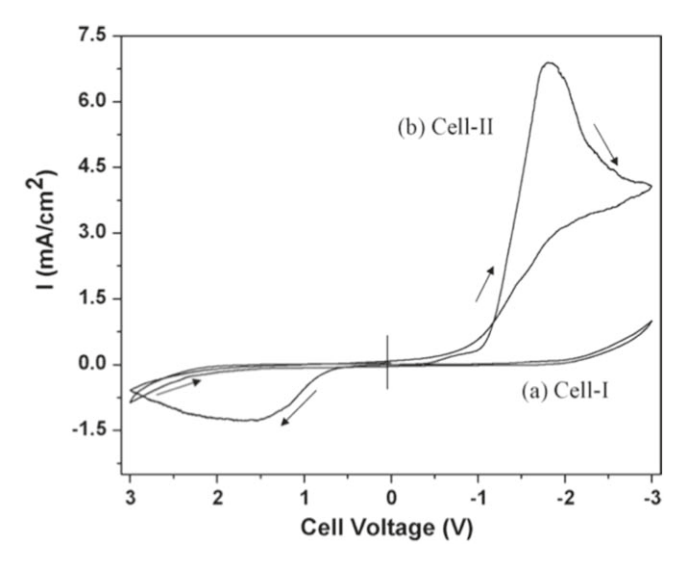


Figure 7. Cyclic voltammograms of (a) cell-I: SS|GPE|SS, and (b) cell-II: Mg|GPE|Mg; recorded at room temperature at a scan rate of $5 \, \text{m V s}^{-1}$. (Reprinted from Ref. 147).

three orders of magnitude higher than that of $PEO-Mg(ClO_4)_2^{84}$ due to the iconicity of the IL and completely amorphous structure of the GPE.

Single Ion Conductors and Cation Only Conductors

The first magnesium single ion conductor, magnesium poly (phosphazene sulfonate), was reported by Chen and colleagues. 157 Ionic conductivity at 50 °C was $10^{-6}\,\mathrm{S}~\mathrm{cm}^{-1}$ with additive cryptand, while further electrochemical testing was not conducted. Another type of single ion conductor, Nafion-117, with different counter cations (including Mg) has been investigated in both aqueous solution and non-aqueous solutions. $^{158-160}$ The ionic conductivity of the magnesiated form was above $10^{-3}\,\mathrm{S}~\mathrm{cm}^{-1}$ at optimum concentration in aqueous media.

Magnesium single ion conducting polymers were more recently reconsidered in 2016 by Balsara and colleagues. ¹⁶¹ They investigated PEO and poly[(styrene-4-sulfonyl trifluoromethyl sulfonyl) imide lithium] P[(STFSI)₂Mg] block copolymers; structures are shown in Fig. 8. ¹⁶¹ The ionic conductivity of the magnesiated polymer was $\sim 3 \times 10^{-7}$ S cm⁻¹ at 50 °C, more than an order of magnitude lower than the corresponding lithiated polymer. Small angle X-ray scattering (SAXS) indicated that the lower ionic

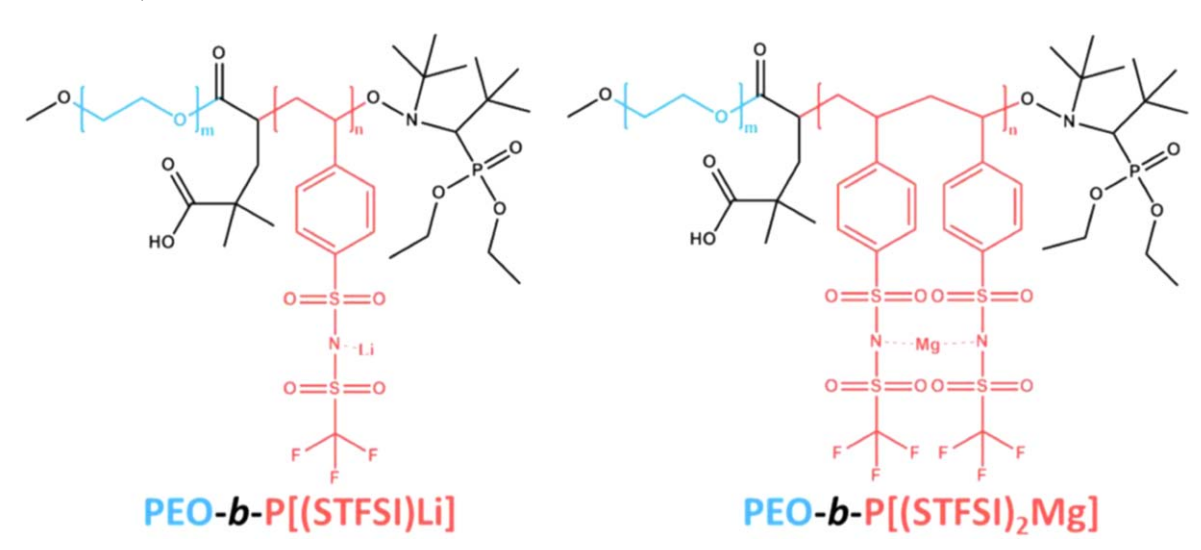


Figure 8. Chemical structure for Li and Mg types of single-ion block copolymers. (Reprinted (adapted) with permission from Ref. ¹⁶¹ Copyright (2016) American Chemical Society.).

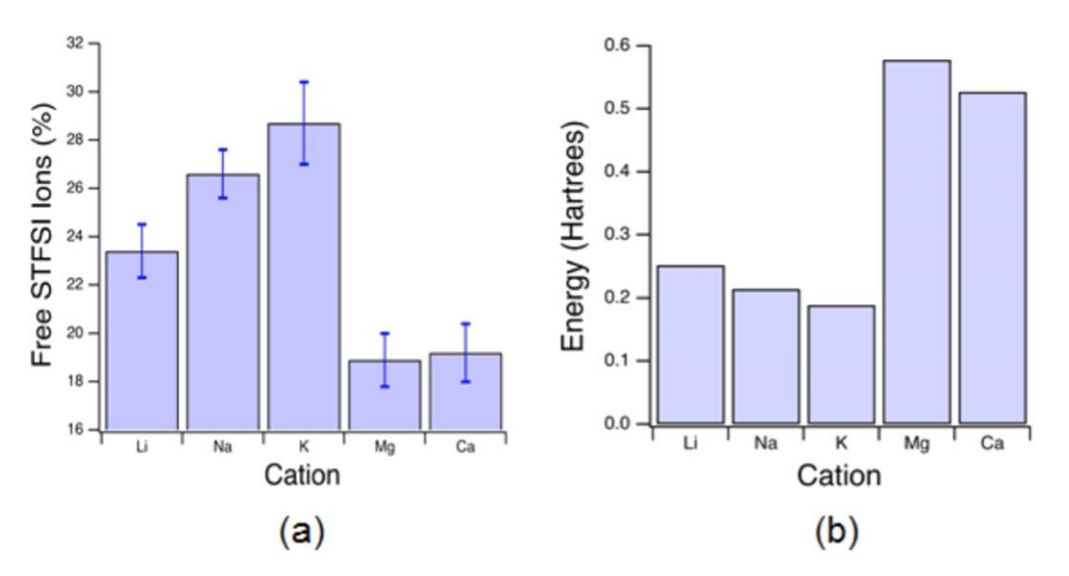


Figure 9. (a) Measured free ion percentages from Raman spectroscopy for PEG31DA-x-STFSIX electrolytes, and (b) DFT predicted dissociation energies for STFSIX ion pairs. X is the variable cation. (Reprinted from Ref. 162).

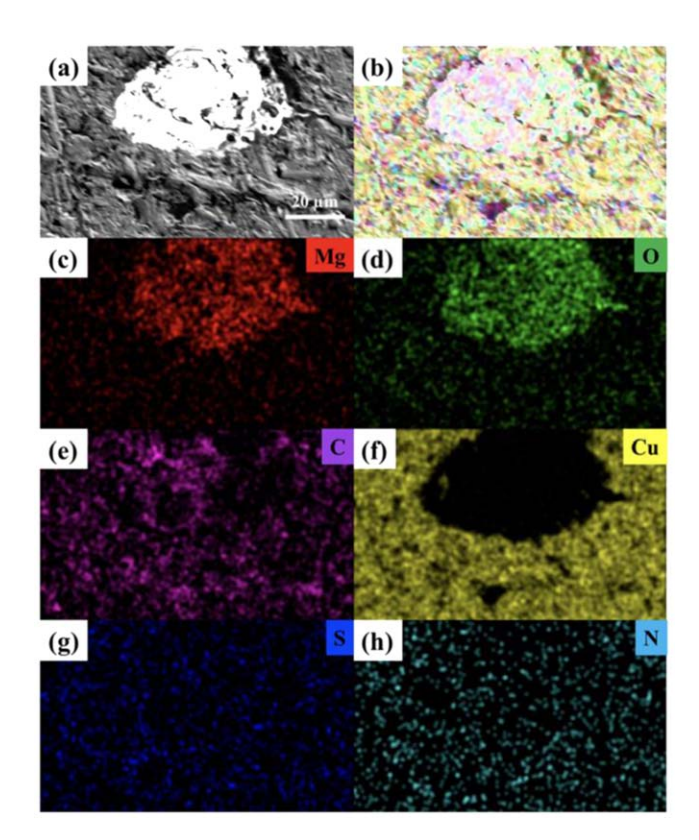


Figure 10. SEM image of copper electrode surface after polarization test at 80 °C (a) and corresponding EDS elemental mapping (b)–(h). (Reprinted (adapted) with permission from Ref. 163 Copyright (2019) American Chemical Society.).

conductivity was due to the lack of ion dissociation in PEO-P[(STFSI)₂Mg]. Raman and DFT studies on poly(ethylene glycol) diacrylate (PEGDA)-STFSIX (X = Li, Na, K, Mg, Ca) electrolytes by Schaefer and colleagues indicated a smaller portion of "free" (uncoordinated) anions and higher dissociation energies for divalent cations, as shown in Fig. 9. 162

Crosslinked gel polymer single ion conductors based on PEGDMA-STFSIMg were further investigated by swelling in

different solvent mixtures.³⁶ Single-ion conducting GPEs swelled in solvent mixtures containing 10% DMSO achieved ionic conductivities of greater than 10⁻⁴ S cm⁻¹. Sparse magnesium metal deposits on the Cu current collector surface were observed with the GPEs swelled in DME/DMSO mixtures after potentiostatic polarization of a Mg/Cu cell. It was not conclusively determined if Mg electrodissolution or electrodeposition hindered the transport of Mg from the source to the current collector.

Solvent-free, dual cation exchanged polymerized ionic liquids based on PSTFSI, with counter cations ${\rm Mg}^{2+}$ and ${\rm BMI}^+$, were investigated; this dual cation exchanged polyionic liquid did not contain free (unpolymerized) anions. 163 Ionic conductivity of BMIPSTFSI was observed as $10^{-7}~{\rm S~cm}^{-1}$ at 20 °C and only minor decreases in total conductivity were found with the addition of up to 5 mol% Mg(PSTFSI)2. Via SAXS, changes to structure were observed above 5 mol% Mg(PSTFSI)2, where the ionic conductivity began to decrease. Finite Mg ion conduction was confirmed as small particle-like magnesium deposits were observed on Cu after polarization of a Mg/Cu cell at elevated temperatures, as shown in Fig. 10, however, facile electrodissolution/electrodeposition was not observed.

Biopolymers

Biopolymers are polymers that are available from natural sources (e.g. living organisms) and have advantages including sustainability, low cost, and biodegradability. ¹⁶⁴ Recently, biopolymers such as agar, ¹⁶⁵ iota-carrageenan, ^{166–168} chitosan, ^{169,170} cellulose acetate, ¹⁷¹ starch/glycerin, ¹⁷² pectin, ¹⁷³ and tamarind seed polysaccharide (TSP) ¹⁷⁴ have been considered as host materials for Mg conducting polymer electrolytes. The reported ionic conductivity and selected other properties of the magnesium biopolymer electrolytes are summarized in Table V. Importantly, biopolymers contain high quantities of proton-labile functional groups such as –OH, –COOH, etc.; these functionalities are subject to reaction with a pristine magnesium metal interface.

Conclusions

Despite dozens of reports of magnesium polymer electrolytes, there is a dearth of investigations of such electrolytes that facilitate reversible and efficient electrochemistry with magnesium metal anodes. Achieving positive results with magnesium GPEs is arguably much easier than with magnesium SPEs, due to existing

Table V. Ionic conductivity and other properties of biopolymer based Mg-conducting electrolytes. T_g in parentheses are for pure polymers. Ionic conductivity in parentheses are optimum ionic conductivity without IL. MTATFSI: methyl-trioctylammonium bis(trifluoromethyl sulfonyl)imide.

Host materials	Mg salt	Additives	Ionic conductivity (S cm ⁻²)	Other properties	References
Agar	Mg(Tf) ₂	_	10 ⁻⁶ (30 °C)	TGA	165
				>200 °C	
				(5% mass loss)	
Iota-carrageenan	$Mg(NO_3)_2$	_	6.1×10^{-4}	$T_g = 75$ °C	167
				(45 °C)	
	$Mg(ClO_4)_2$	_	2.18×10^{-3}	$T_g = 43 ^{\circ}C$	166
	$Mg(Tf)_2$	MTATFSI	3.20×10^{-3}	_	168
			(1.24×10^{-6})		
Chitosan	$Mg(Tf)_2$	EMITf	3.57×10^{-5}	Mg Mg CV, overpotential \sim 2 V	169
			(1.25×10^{-6})		
			(10 wt% salt)		
	$Mg(Tf)_2$	_	9.58×10^{-5}	_	170
			(50 wt% salt)		
TSP	$Mg(ClO_4)_2$	_	5.66×10^{-4}	_	174
Pectin	$Mg(NO_3)_2$	_	7.70×10^{-4}	$T_g = 58$ °C	173
	-			(44 °C)	
Corn starch	$MgSO_4$	_	8.52×10^{-5}	<u> </u>	172
Cellulose acetate	$Mg(ClO_4)_2$	_	4.05×10^{-4}	$T_{\rm g}=65~{ m ^{\circ}C}$	171
	-			(83 °C)	

knowledge of the efficiency of Mg electrodeposition and dissolution from various liquid magnesium electrolytes. Advances are not expected via borrowing of materials approaches from the lithium metal polymer battery literature due to the distinct differences between lithium metal and magnesium metal electrochemistry. Thus, there is a tremendous opportunity for polymer electrolyte researchers to enable new rechargeable magnesium metal polymer batteries, either through the design of new magnesium conducting polymer matrices with both stability and support of Mg metal electrodeposition/dissolution or through the engineering of artificial SEIs on Mg metal that enable stability and reversibility with a broader range of magnesium conducting polymer electrolyte chemistries. A successful configuration must support high Coulombic efficiency and uniform, non-dendritic morphology at the anode upon extended cycling. We strongly urge researchers to consider compatibility with the Mg metal anode when developing future magnesium polymer electrolytes and to perform and report the necessary characterization such that compatibility and true reversibility may be fairly assessed.

Acknowledgments

The authors gratefully acknowledge financial support from the National Science Foundation through award numbers DMR-1654162 and CBET-1706370 and from the University of Notre Dame.

ORCID

Bumjun Park https://orcid.org/0000-0002-3779-1315 Jennifer L. Schaefer https://orcid.org/0000-0003-4293-6328

References

- 1. K. Rhoads and C. L. Sanders, Environ. Res., 36, 359 (1985).
- 2. C. B. Bucur, T. Gregory, A. G. Oliver, and J. Muldoon, J. Phys. Chem. Lett., 6, 3578 (2015).
- 3. H. D. Yoo, I. Shterenberg, Y. Gofer, G. Gershinsky, N. Pour, and D. Aurbach, Energy Environ. Sci., 6, 2265 (2013).
- 4. P. Saha, M. K. Datta, O. I. Velikokhatnyi, A. Manivannan, D. Alman, and P. N. Kumta, *Prog. Mater Sci.*, **66**, 1 (2014).
- 5. F. J. Millero, R. Feistel, D. G. Wright, and T. J. McDougall, Deep Sea Res. Part I Oceanogr. Res. Pap., 55, 50 (2008).
- 6. I. Shterenberg, M. Salama, Y. Gofer, E. Levi, and D. Aurbach, MRS Bull., 39, 453 (2014)
- J. Muldoon, C. B. Bucur, A. G. Oliver, T. Sugimoto, M. Matsui, H. S. Kim, G. D. Allred, J. Zajicek, and Y. Kotani, Energy Environ. Sci., 5, 5941 (2012).
- 8. M. S. Park, J. G. Kim, Y. J. Kim, N. S. Choi, and J. S. Kim, Isr. J. Chem., 55, 570 (2015)
- 9. J. Muldoon, C. B. Bucur, and T. Gregory, Angew. Chemie Int. Ed., 56, 12064
- 10. A. Ponrouch and M. R. Palacín, Phil. Trans. R. Soc., 377 (2019).
- 11. R. Mohtadi and F. Mizuno, Beilstein J. Nanotechnol., 5, 1291 (2014).
- 12. O. Tutusaus and R. Mohtadi, ChemElectroChem, 2, 51 (2015).
- 13. J. Song, E. Sahadeo, M. Noked, and S. B. Lee, J. Phys. Chem. Lett., 7, 1736 (2016)
- 14. R. Deivanayagam, B. J. Ingram, and R. Shahbazian-Yassar, Energy Storage Mater., 21, 136 (2019).
- 15. M. Matsui, J. Power Sources, 196, 7048 (2011).
- 16. C. Ling, D. Banerjee, and M. Matsui, Electrochim. Acta, 76, 270 (2012).
- 17. M. Jäckle and A. Groß, J. Chem. Phys., 141, 174710 (2014).
- 18. M. Jäckle, K. Helmbrecht, M. Smits, D. Stottmeister, and A. Groß, Energy Environ. Sci., 11, 3400 (2018).
- 19. T. D. Gregory, R. J. Hoffman, and R. C. Winterton, J. Electrochem. Soc., 137, 775
- 20. R. Davidson et al., ACS Energy Lett., 4, 375 (2019).
- 21. R. Davidson et al., Mater. Horiz., 7, 843 (2020).
- 22. M. S. Ding, T. Diemant, R. J. Behm, S. Passerini, and G. A. Giffin, J. Electrochem. Soc., 165, A1983 (2018).
- 23. M. Armand, Solid State Ionics, 9-10, 745 (1983).
- 24. M. B. Armand, Annu. Rev. Mater. Sci., 16, 245 (1986).
- 25. M. Armand, *Solid State Ionics*, **69**, 309 (1994).
- 26. D. Baril, C. Michot, and M. Armand, Solid State Ionics, 94, 35 (1997).
- 27. J. Mindemark, M. J. Lacey, T. Bowden, and D. Brandell, Prog. Polym. Sci., 81, 114 (2018).
- 28. I. Gracia, M. Armand, and D. Shanmukaraj, , ed. R. Murugan and W. Weppner (Springer International Publishing, Cham) p. 347 (2019).
- 29. B. Scrosati and C. A. Vincent, MRS Bull., 25, 28 (2000).
- 30. B. Scrosati, F. Croce, and S. Panero, J. Power Sources, 100, 93 (2001).

- 31. V. Di Noto, S. Lavina, G. A. Giffin, E. Negro, and B. Scrosati, *Electrochim. Acta*, 57, 4 (2011).
- 32. A. Mauger, M. Armand, C. M. Julien, and K. Zaghib, J. Power Sources, 353, 333 (2017)
- 33. A. Arya and A. L. Sharma, *Ionics (Kiel).*, 23, 497 (2017).
- 34. H. Zhang, C. Li, M. Piszcz, E. Coya, T. Rojo, L. M. Rodriguez-Martinez, M. Armand, and Z. Zhou, Chem. Soc. Rev., 46, 797 (2017).
- 35. N. S. Schauser, R. Seshadri, and R. A. Segalman, Mol. Syst. Des. Eng., 4, 263 (2019)
- 36. L. C. Merrill, H. O. Ford, and J. L. Schaefer, ACS Appl. Energy Mater., 2, 6355 (2019).
- 37. L. C. Merrill and J. L. Schaefer, Front. Chem., 7, 194 (2019).
- 38. L. C. Merrill and J. L. Schaefer, Chem. Mater., 30, 3971 (2018).
- K. Xu, Chem. Rev., 114, 11503 (2014).
- 40. N. N. Rajput, X. Qu, N. Sa, A. K. Burrell, and K. A. Persson, J. Am. Chem. Soc., **137**, 3411 (2015).
- 41. K. Shimokawa, H. Matsumoto, and T. Ichitsubo, J. Phys. Chem. Lett., 9, 4732 (2018).
- 42. H. D. Yoo, S.-D. Han, I. L. Bolotin, G. M. Nolis, R. D. Bayliss, A. K. Burrell, J. T. Vaughey, and J. Cabana, *Langmuir*, 33, 9398 (2017).
- 43. T. Mandai, K. Tatesaka, K. Soh, H. Masu, A. Choudhary, Y. Tateyama, R. Ise, H. Imai, T. Takeguchi, and K. Kanamura, Phys. Chem. Chem. Phys., 21, 12100 (2019).
- 44. Z. Zhao-Karger, M. E. Gil Bardaji, O. Fuhr, and M. Fichtner, J. Mater. Chem. A, 5, 10815 (2017).
- O. Tutusaus, R. Mohtadi, T. S. Arthur, F. Mizuno, E. G. Nelson, and Y. V. Sevryugina, Angew. Chemie Int. Ed., 54, 7900 (2015).
- 46. S. G. McArthur, L. Geng, J. Guo, and V. Lavallo, Inorg. Chem. Front., 2, 1101 (2015).
- 47. J. Luo, Y. Bi, L. Zhang, X. Zhang, and T. L. Liu, Angew. Chemie Int. Ed., 58, 6967 (2019).
- S.-B. Son, T. Gao, S. P. Harvey, K. X. Steirer, A. Stokes, A. Norman, C. Wang, A. Cresce, K. Xu, and C. Ban, Nat. Chem., 10, 532 (2018).
- 49. M. Marcinek et al., Solid State Ionics, 276, 107 (2015).
- 50. K. A. See, K. W. Chapman, L. Zhu, K. M. Wiaderek, O. J. Borkiewicz, C. J. Barile, P. J. Chupas, and A. A. Gewirth, J. Am. Chem. Soc., 138, 328 (2016).
- 51. G. Bieker, M. Salama, M. Kolek, Y. Gofer, P. Bieker, D. Aurbach, and M. Winter, ACS Appl. Mater. Interfaces, 11, 24057 (2019).
- 52. N. Pour, Y. Gofer, D. T. Major, and D. Aurbach, J. Am. Chem. Soc., 133, 6270 (2011).
- 53. N. N. Rajput, T. J. Seguin, B. M. Wood, X. Qu, and K. A. Persson, Top. Curr. Chem., 376, 19 (2018).
- 54. J. Evans, C. A. Vincent, and P. G. Bruce, *Polymer (Guildf).*, 28, 2324 (1987).
- 55. P. G. Bruce, J. Evans, and C. A. Vincent, Solid State Ionics, 28-30, 918 (1988).
- H. J. Walls and T. A. Zawodzinski, Electrochem. Solid-State Lett., 3, 321 (2000). 57. S. A. Krachkovskiy, J. M. Foster, J. D. Bazak, B. J. Balcom, and G. R. Goward,
- Phys. Chem. C, 122, 21784 (2018).
- 58. F. Schmidt, A. Pugliese, C. C. Santini, F. Castiglione, and M. Schönhoff, Magn. Reson. Chem., 58, 271 (2019).
- 59. M. P. Rosenwinkel and M. Schönhoff, J. Electrochem. Soc., 166, A1977 (2019).
- K. Hayamizu, S. Seki, H. Miyashiro, and Y. Kobayashi, J. Phys. Chem. B, 110, 22302 (2006)
- 61. T. P. Hanusa, Encyclopedia of Inorganic and Bioinorganic Chemistry, ed. R. A. Scott (John Wiley & Sons, New Jersey) (2015).
- 62. R. Dugas, J. D. Forero-Saboya, and A. Ponrouch, *Chem. Mater.*, 31, 8613 (2019).
- Y. Shao et al., Nano Energy, 12, 750 (2015).
- 64. O. Chusid, Y. Gofer, H. Gizbar, Y. Vestfrid, E. Levi, D. Aurbach, and I. Riech, Adv. Mater., 15, 627 (2003).
- 65. A. Du, H. Zhang, Z. Zhang, J. Zhao, Z. Cui, Y. Zhao, S. Dong, L. Wang, X. Zhou, and G. Cui, Adv. Mater., 31, 1805930 (2019).
- 66. M. Mao, T. Gao, S. Hou, and C. Wang, Chem. Soc. Rev., 47, 8804 (2018).
- 67. Z. Zhao-Karger and M. Fichtner, Front. Chem., 6, 656 (2019).
- 68. P. J. Pallister, I. L. Moudrakovski, and J. A. Ripmeester, Phys. Chem. Chem. Phys., 11, 11487 (2009).
- J. C. C. Freitas and M. E. Smith, G. A. B. T.-A. R. on N. M. R. S. Webb (Academic Press, New York) 75, 25 (2012).
- 70. J. Z. Hu et al., *Nano Energy*, **46**, 436 (2018).
- 71. Y. Yang, Y. Qiu, Y. NuLi, W. Wang, J. Yang, and J. Wang, J. Mater. Chem. A, 7, 18295 (2019).
- C. Liao et al., *J. Mater. Chem. A*, 3, 6082 (2015).
 S.-Y. Ha, Y.-W. Lee, S. W. Woo, B. Koo, J.-S. Kim, J. Cho, K. T. Lee, and N.-S. Choi, ACS Appl. Mater. Interfaces, 6, 4063 (2014).
- 74. T. Watkins and D. A. Buttry, J. Phys. Chem. B, 119, 7003 (2015).
- 75. M. Kar, Z. Ma, L. M. Azofra, K. Chen, M. Forsyth, and D. R. MacFarlane, Chem. Commun., 52, 4033 (2016).
- 76. M. Armand, J. M. Chabagno, and M. Duclot, Second International Meeting on Solid State Electrolytes, St. Andrews, Scotland, 2309, 5 (1978).
- M. B. Armand et al., Electrodes and Electrolytes, North Holland, Amsterdam 21-25th May, 1979131 (1979).
- 78. L. L. Yang, A. R. McGhie, and G. C. Farrington, J. Electrochem. Soc., 133, 1380 (1986).
- 79. A. Bakker, S. Gejji, J. Lindgren, K. Hermansson, and M. M. Probst, Polymer (Guildf)., 36, 4371 (1995).
- 80. S. Ramalingaiah, D. S. Reddy, M. J. Reddy, E. Laxminarsaiah, and U. V. S. Rao, Mater. Lett., 29, 285 (1996).

- K. M. Anilkumar, B. Jinisha, M. Manoj, and S. Jayalekshmi, *Eur. Polym. J.*, 89, 249 (2017).
- 82. J. L. Acosta and E. Morales, *Electrochim. Acta*, 43, 791 (1998).
- R. C. Agrawal, D. K. Sahu, Y. K. Mahipal, and R. Ashrafi, *Mater. Chem. Phys.*, 139, 410 (2013).
- 84. M. Jaipal Reddy and P. P. Chu, J. Power Sources, 109, 340 (2002).
- M. A. K. L. Dissanayake, L. R. A. K. Bandara, L. H. Karaliyadda, P. A. R. D. Jayathilaka, and R. S. P. Bokalawala, *Solid State Ionics*, 177, 343 (2006).
- A. R. Polu, R. Kumar, K. V. Kumar, and N. K. Jyothi, AIP Conf. Proc., 1512, 996 (2013).
- 87. S.-K. Jeong, Y.-K. Jo, and N.-J. Jo, *Electrochim. Acta*, 52, 1549 (2006).
- 88. A. R. POLU and R. KUMAR, Bull. Mater. Sci., 34, 1063 (2011).
- 89. A. R. Polu and R. Kumar, Chinese J. Polym. Sci., 31, 641 (2013).
- A. R. Polu, R. Kumar, K. V. Kumar, and N. K. Jyothi, AIP Conf. Proc., 1512, 996 (2013).
- M. Ramaswamy, T. Malayandi, S. Subramanian, J. Srinivasalu, and M. Rangaswamy, *Ionics (Kiel).*, 23, 1771 (2017).
- R. Manjuladevi, M. Thamilselvan, S. Selvasekarapandian, R. Mangalam, M. Premalatha, and S. Monisha, *Solid State Ionics*, 308, 90 (2017).
- R. Manjuladevi, S. Selvasekarapandian, M. Thamilselvan, R. Mangalam, S. Monisha, and P. C. Selvin, *Ionics (Kiel).*, 24, 3493 (2018).
- 94. A. A. Aziz and Y. Tominaga, Ionics (Kiel)., 24, 3475 (2018).
- 95. A. A. Aziz and Y. Tominaga, *Polym. J.*, **51**, 61 (2019).
- 96. S. Ramesh, S. C. Lu, and E. Morris, J. Taiwan Inst. Chem. Eng., 43, 806 (2012).
- 97. S. Ponmani and M. R. Prabhu, *J. Mater. Sci., Mater. Electron.*, **29**, 15086 (2018).
- 98. S. P. Nidhi and R. Kumar, J. Alloys Compd., 789, 6 (2019).
- L.-L. Yang, R. Huq, G. C. Farrington, and G. Chiodelli, Solid State Ionics, 18–19, 291 (1986).
- A. Patrick, M. Glasse, R. Latham, and R. Linford, Solid State Ionics, 18–19, 1063 (1986).
- J. Y. Cherng, M. Z. A. Munshi, B. B. Owens, and W. H. Smyrl, *Solid State Ionics*, 28–30, 857 (1988).
- 102. J. Shi and C. A. Vincent, Solid State Ionics, 60, 11 (1993).
- 103. C. A. Vincent, *Electrochim. Acta*, 40, 2035 (1995).
- A. R. Polu, R. Kumar, V. Causin, and R. Neppalli, J. Korean Phys. Soc., 59, 114 (2011).
- 105. A. R. Polu, R. Kumar, and H. W. Rhee, High Perform. Polym., 26, 628 (2014).
- R. Mohtadi, M. Matsui, T. S. Arthur, and S.-J. Hwang, *Angew. Chemie Int. Ed.*, 51, 9780 (2012).
- H. A. Every, F. Zhou, M. Forsyth, and D. R. MacFarlane, *Electrochim. Acta*, 43, 1465 (1998).
- F. B. Dias, S. V. Batty, G. Ungar, J. P. Voss, and P. V. Wright, J. Chem. Soc. Faraday Trans., 92, 2599 (1996).
- 109. F. B. Dias, S. V. Batty, A. Gupta, G. Ungar, J. P. Voss, and P. V. Wright, *Electrochim. Acta*, 43, 1217 (1998).
- 110. C. Liebenow, *Electrochim. Acta*, 43, 1253 (1998)
- 111. C. Liebenow, Solid State Ionics, 136-137, 1211 (2000).
- D. Aurbach, Z. Lu, A. Schechter, Y. Gofer, H. Gizbar, R. Turgeman, Y. Cohen, M. Moshkovich, and E. Levi, *Nature*, 407, 724 (2000).
- H. O. Ford, L. C. Merrill, P. He, S. P. Upadhyay, and J. L. Schaefer, *Macromolecules*, 51, 8629 (2018).
- V. D. Noto, S. Lavina, D. Longo, and M. Vidali, *Electrochim. Acta*, 43, 1225 (1998).
- 115. V. Di Noto and M. Vittadello, *Solid State Ionics*, **147**, 309 (2002).
- M. Saito, H. Ikuta, Y. Uchimoto, M. Wakihara, S. Yokoyama, T. Yabe, and M. Yamamoto, J. Phys. Chem. B, 107, 11608 (2003).
- M. Saito, H. Ikuta, Y. Uchimoto, M. Wakihara, S. Yokoyama, T. Yabe, and M. Yamamoto, J. Electrochem. Soc., 150, A726 (2003).
- M. Saito, H. Ikuta, Y. Uchimoto, M. Wakihara, S. Yokoyama, T. Yabe, and M. Yamamoto, J. Electrochem. Soc., 150, A477 (2003).
- N. H. Zainol, S. M. Samin, L. Othman, K. B. M. Isa, W. G. Chong, and Z. Osman, Int. J. Electrochem. Sci., 8, 3602 (2013).
- 120. G. G. Kumar and N. Munichandraiah, Electrochim. Acta, 44, 2663 (1999).
- 121. G. G. Kumar and N. Munichandraiah, Solid State Ionics, 128, 203 (2000).
- 122. G. G. Kumar and N. Munichandraiah, J. Power Sources, 91, 157 (2000).
- 123. G. Girish Kumar and N. Munichandraiah, J. Electroanal. Chem., 495, 42 (2000).
- 124. G. Girish Kumar and N. Munichandraiah, J. Power Sources, 102, 46 (2001).
- 125. G. Girish Kumar and N. Munichandraiah, Electrochim. Acta, 47, 1013 (2002)
- K. Perera, M. A. K. Dissanayake, and P. W. S. Bandaranayake, *Mater. Res. Bull.*, 39, 1745 (2004).
- 127. J.-S. Oh, J.-M. Ko, and D.-W. Kim, *Electrochim. Acta*, 50, 903 (2004).
- G. P. Pandey, R. C. Agrawal, and S. A. Hashmi, J. Power Sources, 190, 563 (2009).
- 129. G. P. Pandey, R. C. Agrawal, and S. A. Hashmi, J. Phys. D: Appl. Phys., 43, 255501 (2010).

- G. P. Pandey, R. C. Agrawal, and S. A. Hashmi, J. Solid State Electrochem., 15, 2253 (2011)
- G. P. Pandey, R. C. Agrawal, and S. A. Hashmi, J. Phys. Chem. Solids, 72, 1408 (2011).
- 132. J. Sharma and S. Hashmi, *Polym. Compos.*, 40, 1295 (2019).
- N. Yoshimoto, S. Yakushiji, M. Ishikawa, and M. Morita, *Electrochim. Acta*, 48, 2317 (2003).
- S. N. Asmara, M. Z. Kufian, S. R. Majid, and A. K. Arof, *Electrochim. Acta*, 57, 91 (2011).
- K. A. J. K. Karunarathne, K. S. Perera, K. P. Vidanapathirana, and J. C. Pitawela, J. Solid State Electrochem., 23, 2165 (2019).
- S. K. Tripathi, A. Jain, A. Gupta, and M. Mishra, J. Solid State Electrochem., 16, 1799 (2012).
 S. K. Tripathi, A. Gupta, A. Jain, and M. Kumari, Indian J. Pure Appl. Phys., 51,
- 358–61 (2013), http://nopr.niscair.res.in/handle/123456789/17688.
- 138. J. Sharma and S. A. Hashmi, J. Solid State Electrochem., 17, 2283 (2013).
- E. Sheha, M. M. Nasr, and M. K. El-Mansy, *Mater. Sci. Technol.*, 31, 1113 (2015).
 D. Hambali, Z. Zainuddin, and Z. Osman, *Ionics (Kiel).*, 23, 285 (2017).
- D. Hambali, N. H. Zainol, L. Othman, K. B. Md Isa, and Z. Osman, *lonics (Kiel).*, 25, 1187 (2019).
- H. Ohno, Electrochemical Aspects of Ionic Liquids (John Wiley & Sons, Ltd, New Jersey) (2005).
- D. R. MacFarlane, M. Forsyth, P. C. Howlett, J. M. Pringle, J. Sun, G. Annat, W. Neil, and E. L. Izgorodina, Acc. Chem. Res., 40, 1165 (2007).
- W. Neil, and E. I. Izgorodina, Acc. Chem. Res., 40, 1165 (2007).
 144. M. Galiński, A. Lewandowski, and I. Stępniak, Electrochim. Acta, 51, 5567
- (2006). 145. N. Yoshimoto, T. Shirai, and M. Morita, *Electrochim. Acta*, **50**, 3866 (2005).
- M. Morita, T. Shirai, N. Yoshimoto, and M. Ishikawa, J. Power Sources, 139, 351 (2005).
- 147. G. P. Pandey and S. A. Hashmi, J. Power Sources, 187, 627 (2009).
- X. Tang, R. Muchakayala, S. Song, Z. Zhang, and A. R. Polu, *J. Ind. Eng. Chem.*, 37, 67 (2016).
- 149. J. Sharma and S. A. Hashmi, Bull. Mater. Sci., 41, 147 (2018).
- 150. J. Wang, Z. Zhao, R. Muchakayala, and S. Song, J. Memb. Sci., 555, 280 (2018).
- V. Aravindan, G. Karthikaselvi, P. Vickraman, and S. P. Naganandhini, J. Appl. Polym. Sci., 112, 3024 (2009).
- 152. S. Ponmani and M. R. Prabhu, *Polym. Technol. Mater.*, **58**, 978 (2019).
- 153. Y. Kumar, S. A. Hashmi, and G. P. Pandey, *Electrochim. Acta*, 56, 3864 (2011).
- 154. G. P. Pandey, Y. Kumar, and S. A. Hashmi, *Solid State Ionics*, **190**, 93 (2011).
- H. N. M. Sarangika, M. A. K. L. Dissanayake, G. K. R. Senadeera, R. R. D. V. Rathnayake, and H. M. J. C. Pitawala, *Ionics (Kiel).*, 23, 2829 (2017).
- S. Song, M. Kotobuki, F. Zheng, Q. Li, C. Xu, Y. Wang, W. D. Z. Li, N. Hu, and L. Lu, J. Electrochem. Soc., 164, A741 (2017).
- 57. K. Chen and D. F. Shriver, *Chem. Mater.*, **3**, 771 (1991).
- 158. S. T. Iyer, D. Nandan, and B. Venkataramani, React. Funct. Polym., 29, 51 (1996).
- G. Pourcelly, A. Oikonomou, C. Gavach, and H. D. Hurwitz, *J. Electroanal. Chem. Interfacial Electrochem.*, 287, 43 (1990).
 M. Doyle, M. E. Lewittes, M. G. Roelofs, S. A. Perusich, and R. E. Lowrey,
- M. Doyle, M. E. Lewittes, M. G. Roelofs, S. A. Perusich, and R. E. Lowrey, J. Memb. Sci., 184, 257 (2001).
- J. L. Thelen, S. Inceoglu, N. R. Venkatesan, N. G. Mackay, and N. P. Balsara, *Macromolecules*, 49, 9139 (2016).
- 162. C. T. Elmore, M. E. Seidler, H. O. Ford, L. C. Merrill, S. P. Upadhyay, W. F. Schneider, and J. L. Schaefer, *Batteries*, 4, 1 (2018).
- B. Park, H. O. Ford, L. C. Merrill, J. Liu, L. P. Murphy, and J. L. Schaefer, ACS Appl. Polym. Mater., 1, 2907 (2019).
- N. F. Ab. Rahman, L. K. Shyuan, A. B. Mohamad, and A. A. H. Kadhum, *Appl. Mech. Mater.*, 291–294, 614 (2013).
- R. D. Alves, L. C. Rodrigues, J. R. Andrade, A. Pawlicka, L. Pereira, R. Martins, E. Fortunato, and M. M. Silva, Mol. Cryst. Liq. Cryst., 570, 1 (2013).
- S. Shanmuga Priya, M. Karthika, S. Selvasekarapandian, R. Manjuladevi, and S. Monisha, *Ionics (Kiel).*, 24, 3861 (2018).
- S. S. Priya, M. Karthika, S. Selvasekarapandian, and R. Manjuladevi, Solid State Ionics, 327, 136 (2018).
- 168. N. K. Farhana, F. S. Omar, R. Shanti, Y. K. Mahipal, S. Ramesh, and K. Ramesh, *Ionics (Kiel)*, 25, 3321 (2019).
- 169. J. Wang, S. Song, S. Gao, R. Muchakayala, R. Liu, and Q. Ma, *Polym. Test.*, 62, 278 (2017).
- S. B. Aziz, S. Al-Zangana, H. J. Woo, M. F. Z. Kadir, and O. G. Abdullah, *Results Phys.*, 11, 826 (2018).
- M. Mahalakshmi, S. Selvanayagam, S. Selvasekarapandian, V. Moniha, R. Manjuladevi, and P. Sangeetha, J. Sci. Adv. Mater. Devices, 4, 276 (2019).
- 172. M. F. Hassan and N. S. N. Azimi, *Int. J. Adv. Appl. Sci.*, **6**, 38 (2019).
- 173. S. Kiruthika, M. Malathi, S. Selvasekarapandian, K. Tamilarasan, V. Moniha, and R. Manjuladevi, J. Solid State Electrochem., 23, 2181 (2019).
- P. Perumal, K. P. Abhilash, P. Sivaraj, and P. C. Selvin, *Mater. Res. Bull.*, 118, 110490 (2019).